



Review

Heterogeneous selective oxidation over supported metal catalysts: From nanoparticles to single atoms

Hongling Yang^a, Ganggang Li^b, Guoxia Jiang^{b,*}, Zhongshen Zhang^{b,*}, Zhengping Hao^{b,*}^a Beijing Key Laboratory for VOCs Pollution Prevention and Treatment Technology and Application of Urban Air, Beijing Municipal Research Institute of Eco-Environmental Protection, Beijing 100037, China^b National Engineering Laboratory for VOCs Pollution Control Material & Technology, Research Center for Environmental Material and Pollution Control Technology, University of Chinese Academy of Sciences, Beijing 101408, China

ARTICLE INFO

Keywords:

Heterogeneous selective oxidation catalysis

Nanocatalyst

Single atom catalyst

Activity-structure relationship

ABSTRACT

Selective catalytic oxidation plays a crucial role in both fine chemical and petrochemical industries for the production of significant intermediates, however, it remains challenging to obtain the target product selectively when multiple reaction paths coexist. To overcome this challenge, the recently developed single atom catalysts provide opportunities for highly selective catalytic oxidation, whose catalytic behaviors are distinct from those of nanoclusters and nanoparticles. This review is devoted to summarizing the recent advances in the exploitation of novel catalytic materials (single atoms, nanoclusters and nanoparticles) for four challenging selective oxidation reactions in terms of adsorption, activation and reaction, including selective oxidation of methane, aerobic oxidation of alcohols, epoxidation of alkenes, and preferential oxidation of carbon monoxide in hydrogen. The key factors affecting the catalytic performance, especially the electronic and geometric structures of the single atoms, nanoclusters, and nanoparticles will be discussed. A deep understanding of the active species, active structures, activity-structure relationship and mechanisms for these catalytic systems are highlighted, and the current challenges and future developments are also provided, with the aim to give guidance for the design of efficient and highly selective catalysts for heterogeneous oxidation reactions, and to better understand their catalytic behaviors in a unified way.

1. Introduction

Oxidation catalysis, an indispensable transformation in synthetic chemistry and industrial manufacturing [1,2], contributes over 30 % of the total production in the current chemical industry. Selective oxidation catalysis is the direct route for the production of high-value-added chemicals and intermediates, such as alcohols, epoxides, ketones and aldehydes. Among the selective oxidation processes, the selective oxidation of methane to methanol, acetic acid or C₂ + hydrocarbons, the selective oxidation of alcohols to the corresponding aldehydes/ketones, the selective oxidation of ethylene or propylene to its corresponding epoxides, and the preferential oxidation of CO in hydrogen-rich fuel gas stream are the well-known examples. The key to the selective oxidation relies on the development of efficient and selective catalysts. Based on the already constructed metal catalysts, the established structure-reactivity correlations in performing these reactions provide scientific guidance in understanding the selective oxidation catalysis

[3–6].

So far, apart from enzymatic catalysis [7], two classes of catalysts, that is, homogeneous and heterogeneous catalysts are exploited for the target reactions [8]. The homogeneous catalysts exhibit high selectivity due to their steric and electronic effects, but face the problems of separation and reuse. By contrast, the heterogeneous catalysts show absolute advantage for practical applications in aspects of catalyst separation and recovery. The heterogeneous selective oxidation catalyst has undergone the development of four types of catalysts. The first generation of heterogeneous catalysts are the metal complexes immobilized on oxides [9]. Although high selectivity is obtained, the leaching of metals or ligands is inevitable during selective oxidation reactions because of the weak interaction between metal and support. Later, several covalently bound/anchored metal complexes have demonstrated a remarkable robustness to leaching and hydrolysis/solvolytic [10,11]. With the development of nanoscience, especially nanomaterials, the supported metal nanoparticles are developed as the second-generation catalysts,

* Corresponding authors.

E-mail addresses: jiangguoxia@ucas.ac.cn (G. Jiang), zszhang@ucas.ac.cn (Z. Zhang), zphao@ucas.ac.cn (Z. Hao).<https://doi.org/10.1016/j.apcatb.2023.122384>

Received 29 October 2022; Received in revised form 18 December 2022; Accepted 4 January 2023

Available online 6 January 2023

0926-3373/© 2023 Elsevier B.V. All rights reserved.

yet their selectivity are unsatisfactory due to the side reactions of over-oxidation [12,13]. The nanocatalysts modified with a second metal (Pd, Pt, Na, Sn etc) are regarded as the third-generation heterogeneous catalyst, and their selectivity is greatly improved [14–16].

Understanding the reaction mechanism adjusting its selectivity is prerequisite to rationally design a selective catalyst. So far, there has basically reached an agreement that the selectivity of the catalyst is mainly affected by the adsorption strength and the configuration of the reactants/intermediates on the catalysts surface [8], these in turn depend on the geometric and electronic structures of the active sites. In fact, there are always multiple types of adsorption sites on the surface of heterogeneous catalysts, and multiple adsorption modes of one reactant may exist even though there is only one type of adsorption site. The adsorption modes should depend on the structure and electronic properties of adsorption sites. Some of oxidation reactions may also require the synergy between two or multiple adsorption sites of the catalyst [17, 18]. Therefore, only the substrate is adsorbed on the catalyst surface in a proper pattern, the target product will be obtained with high selectivity. From this point of view, it is not surprising that homogeneous metal complexes show superior selectivity. While in some cases, regioselectivity usually depends on how the oxidant species is able to approach the substrate molecule. It therefore may depend on the influence of the surrounding of the active site with the oxidant, irrespective of the adsorption of the substrate on the site.

Inspired by the homogeneous and enzyme catalysts, the recently emerging single-atom catalysts (SACs) with uniform geometric and electronic structure are regarded as the fourth-generation catalysts [19–21]. Actually, Basset et al. has introduced the concepts of coordination chemistry and homogeneous catalysis into surface science and heterogeneous catalysis in 1980s [22–24]. In 2005, Thomas et al. reported single-site heterogeneous catalysts only have a single type of active site, it is not necessary to be mononuclear [25]. In 2011, Zhang, Li, Liu and co-workers reported that the single Pt atoms dispersed on FeO_x are highly active and stable for CO oxidation [19]. They utilized advanced characterization techniques including high-angle annular dark-field scanning transmission electron microscopy (HAADF-STEM), spectroscopy and density functional theory (DFT) to illuminate the bonding between single Pt atoms and FeO_x support and the catalytic mechanism. And the team proposed the term SAC, which is defined that the metallic active sites of the supported metal catalysts are atomically isolated, and heterogeneous [26]. In fact, the active sites of SAC are not necessarily uniform due to the inhomogeneity of most solid supports, particularly in practical industrial catalysts. Thanks to the mononuclear nature of the active sites, SACs not only possess 100 % atom utilization but also have unique geometric and electronic properties, which are ascribed to the absence of metal-metal bonds and the nature of cationic, and thus tuning the reaction rates and selectivities in various chemical reactions. Therefore, SACs provide an ideal platform to clarify the structure-activity relationship in catalysis at the molecular levels, and they also provide a possibility to link between heterogeneous catalysis and homogeneous catalysis.

It should be pointed out that for multi-molecular activation or reactions requiring multiple active sites, the supported single-site active species are inadequate because of their allowance for only one reactant adsorption mode. Whereas for the supported nanoparticles, their ubiquitous heterogeneity in shape/size/composition results in various catalytic sites so as to satisfy the adsorption and activation of multiple reactants. In addition, compared with supported nanoparticles, the geometric structures of supported single atoms are partially restricted by the support, particularly when supported on inorganic solid supports. Hence, the catalytic applications of single-atom catalysts are mainly focus on the activation of small molecules.

In this review, we summarize the advances in four important and challenging selective oxidation reactions: the oxidation of methane; the aerobic oxidation of alcohols; the epoxidation of alkenes, and CO oxidation catalyzed by supported metal catalysts in the recent 5–10

years. We compare the catalytic performance of nanocatalysts, modified nanocatalysts, and SACs in these four catalytic systems, with an attempt to figure out the critical factors that affect the catalytic activity and selectivity, and further to illuminate the general features shared by good catalysts in respect of electronic and geometric structures of the active sites. We hope that this collection can be instructive in better understanding the metal-catalyzed heterogeneous oxidation reactions.

2. Adsorption of substrates on supported metal nanoparticles and single atoms

The heterogeneous catalytic reaction process includes internal/external diffusion, the chemical adsorption of reactants to generate active intermediates, the active intermediates undergo chemical transformations to generate products, and the desorption of the products. Internal diffusion in and out of the solid catalyst are crucial phases and they often have a key role in determining chemo-, regio- and/or stereoselectivity. Especially, the site confinement and diffusion effects in zeolites [27,28], which are not highlighted in this review. In the reaction controlled by surface reaction, the active sites interact with the substrate to form active intermediates, and thereby lowering the activation energy of the transformations. According to density functional theory (DFT) calculations and in-situ Fourier transform infrared spectrometry (FTIR) studies, there probably exist a variety of intermediates and reaction pathways in a catalytic cycle. The initial step is the adsorption of the substrates on the active sites, which determines the following reaction mechanism and product selectivity.

At present, the adsorption of four substrate molecules including methane, alcohol, alkene and CO has been studied extensively on nanoparticles and SACs, and obtained some consensus conclusions. The edge and corner sites of the CeO_2 nanoparticles favor the adsorption of methane [29]. In 2020, Pantha et al. reported the adsorption energy of methane has a strong and linear correlation with the degree of back-donation of electrons from occupied metal *d*-states to antibonding methane states [30]. Specifically, the interaction between a metal single atom and the oxide support has a great impact on methane adsorption. Jiang et al. found that methane can be strongly chemisorbed on gapped oxides (TiO_2) supported Pt single atom, while methane cannot be chemisorbed on metallic oxides (IrO_2 , RuO_2) supported Pt single atom. This is because the Pt d_z^2 orbital can strongly mix with the electronic states of support-oxide, and become more occupied, then losing its ability to chemisorb methane [31]. The adsorption of alcohols can undergo a two-step process: initial adsorption into the intra-nanoparticle adsorption, followed by that among the inter-nanoparticle adsorption [32]. And the alcohols physisorb on SiO_2 , its binding energies increase with the molecular size of SiO_2 [33]. Shaikhutdinov et al. carried out temperature-programmed desorption (TPD) to observe three adsorption states of ethylene on Pd nanoparticles, multilayer, π -bonded ethylene and interchanging di- σ -bonded ethylene [34], each adsorption state participates in the reaction to obtain specific product. Hulva et al. unraveled CO adsorption on model SACs, and found CO adsorption strength are different at different metal surfaces, the *d*-states of the metal atom and the strength of the metal-CO bond will be modified owing to the charge transfer into the support [35], while bridge-bound CO chains are thermodynamically stable over hollow Pd nanoparticles [36].

The adsorption ability and manner of the substrate rely on the electronic and geometric structure of the active sites (Fig. 1) [37–39], which has been influenced by many factors, including size, shape, composition and coordination environment. Especially, when the size of active metal is reduced to nanoparticles/clusters or even single atoms, their electronic structures will change dramatically, from continuous energy band to discrete energy levels, and finally quantum confinement effect. For instance, the adsorption modes of ethylene relies on the assemblies of metal atoms, on 3-fold metal sites with ethylidyne mode, on the bridges metal dimers with di- σ -mode, and on isolated metal single atoms with π -bonded mode [17].

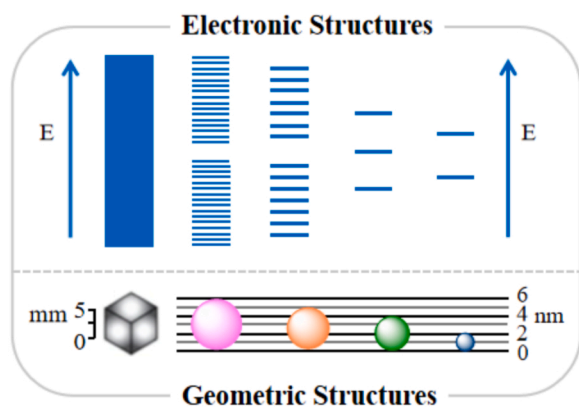


Fig. 1. Electronic and geometric structures of the active sites.

The electronic structures of homogeneous metal complex are strongly dependent on their coordination environment, especially ligands and solvents. Their uniform coordination environment with proper electronic structures results in only one adsorption mode for reactants, thus exhibiting excellent selectivity [40]. There are also some exceptions, if we consider the epoxidation of a dialkene, the interaction of each C=C with the catalytically active site may be identical from an electronic point of view, but the reaction leads to the formation of two completely different epoxides and hence to two different products with low selectivities. However, for supported metal nanoparticles, their heterogeneity in size/shape/composition deriving from the orbital overlapping between metal atoms is ubiquitous [41–44]. In the actual reaction process, the interaction between metal and substrate, and metal and the support should also be considered. These various catalytic sites possess different coordination environments and electronic structures, and will bring about different adsorption strength/patterns of the substrates/intermediates and thereby poor catalytic selectivity. As for the modified nanocatalysts, the introduction of a second metal or surfactant can achieve site modification and isolation via selective poisoning, and thus improving the homogeneity in the active sites, the interaction between each component modify the electronic structure caused by charge transfer, which alters their adsorption behavior and thus regulating the catalytic selectivity [45,46].

In selective oxidation reactions, we hope that the target functional group will be preferentially adsorbed on the active sites. Firstly, the catalyst should have a uniform geometric and electronic structure, which can avoid multiple adsorption modes. Secondly, it should have unique chemical properties, such as redox or acid/alkaline or electrophilic/nucleophilic properties, so that it can efficiently identify target functional groups. When the size of metal species are downsized to nanoscale or even to atomic level, the electronic structures such as work function, surface oxidation states, electronic density of states, band gap will be changed. Particularly, the electronic structures will be remarkably regulated when downsizing to atomically dispersed scale. Thus the bonding/adsorption properties of metal species for substrates and the activation for oxygen molecules will be significantly changed. Moreover, the high homogeneity of single-atom active sites favors confining the adsorption configuration of substrates, which resulting in highly uniform activation process of the reactant molecules. From this perspective, if the active sites are constructed at the atomic level, new catalysts with unexpected catalytic properties are expected to be exploited. Besides, single atom alloy or composite metal catalyst might show their advantages in multiple-step reactions requiring one more type of active sites or the synergy of different active sites.

3. Activation of oxygen molecule and substrate molecules

3.1. Activation of oxygen molecule

The adsorption and activation of molecular oxygen over a catalyst to produce active species is another critical step in heterogeneous oxidation reactions (Fig. 2) [47–49]. According to the Wigner's spin selection rule, the activation of ground-state O_2 into high-energy oxygen species (e.g., O_2 , OH , and 1O_2) are highly desirable for the oxidation reaction [50]. When O_2 is activated, the kinetically stable state of O_2 will be lowered, because its spin-triplet ground state will change and the anti-bonding orbitals will be filled. The activation behavior and the types of active O species (e.g., O_2 , O) and their distribution also have great influence on the catalytic selectivity. In some cases, the presence of some atomic oxygen on the metal surface can raise the O_2 adsorption and dissociation rate, which can be ascribed to the release of metal atoms from surface reconstructing [51].

The molecular oxygen activation on metal nanoparticles, clusters and single sites has been theoretically and experimentally investigated [52–54]. There are three O_2 adsorption modes on the surface of gold nanoparticles, one is a weakly interacting end-on mode, which merely exists on low-coordinated gold atoms on small particles, this adsorption mode is unfavorable from a catalytic point of view. The second is a top-bridge-top mode, which is stable on all gold particles; The third is a bridge-bridge mode, which requires four gold atoms arranging on the gold surface. Metal particle size has a great influence on its adsorption energies, which could reflect the ability of molecular activation towards dissociation. Bridge-bridge conformers possessed the highest degree of molecular activation and the lowest activation barriers for O_2 dissociation [55]. Corma et al. investigated the dissociation of O_2 over Cu_n clusters and nanoparticles with different sizes via DFT calculations, and found an obvious reactivity trend with the atomicity of cluster. The activation energies for the dissociation of O-O bond was less than 10 kcal/mol on small copper nanoparticles (~1 nm diameter), 15–20 kcal/mol on the clusters with 7–10 atoms, more than 40 kcal/mol when n of Cu_n is less than 5.27 [56,57]. These differences in activation behavior towards O_2 lead to difference in the catalytic properties of metal species.

For oxygen adsorption, the electron transfer from the surface to the oxygen molecule is essential [58], and its main influencing factors include oxygen coverage, oxygen vacancy and atom structure or its location on an oxide surface [59]. The activation of O_2 on metal surfaces strongly depends on their electronic, geometry and energetic properties. The degree of O_2 activation can be determined by the coordination number of the metal atoms on the surface. Specifically, the activation of O_2 is much easier over sites with lower coordination numbers than those with more coordinated sites [60,61]. Moreover, metal-support interface [62,63], coadsorbates [64], or basic/aqueous conditions [65] were reported to contribute to the activation of O_2 .

In general, O_2 can behave very differently on various metal surfaces due to the differences in their electronic structure. For example, atomic oxygen is active for olefin epoxidation on Ag and Au surfaces [66–68], while molecular oxygen is active for propylene epoxidation on Cu surfaces [69,70]. Cong et al. reported single-atom Pd sites with partially positive electronic properties showed better ability to activate allylic alcohols and O_2 in comparison with those of nanoparticles [50]. Zhang et al. reported SACs exhibited a higher activity and selectivity for the oxidation of alcohols than the corresponding NP catalysts, because the maximized exposed interfacial sites in SACs promotes the activation of O_2 [71]. Based on the reported literatures, some inert metals are more selective for oxidation, which will be reactive under aerobic conditions, and its selectivity depends on the degree of oxygen coverage on the catalyst surface. Whereas the more reactive metals are usually less selective, but oxygen can passivate their surface, which will increase their selectivity as oxygen coverage increases. Thus, the oxidation state of the surface-bound O_2 might affect its catalytic reactivity and selectivity. The

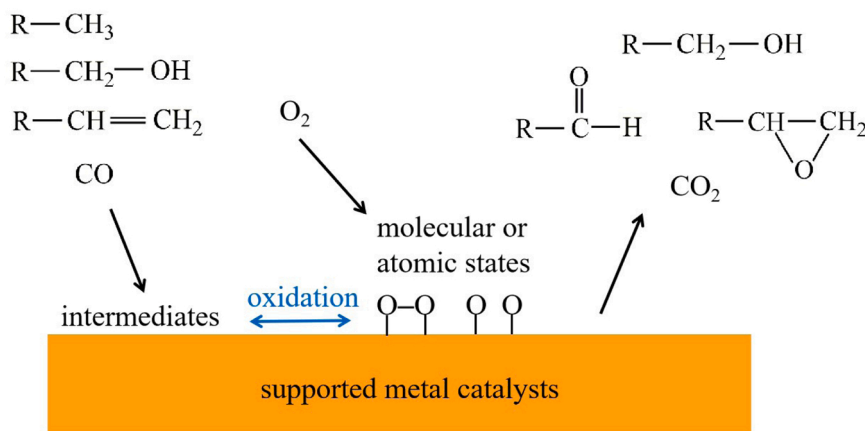


Fig. 2. Schematic of a few important oxidation processes where O_2 activation to adsorbed O_2 or O on metal surface is critical.

activation of molecular oxygen can be achieved by several treatment methods, such as reductive treatment, photolysis [49]. In addition, the type of formed product as a result of an electrophilic attack of oxygen on the hydrocarbon molecule depends on the structure of the oxygen adsorption complex. And the binding of O_2 to the metals surface can also be well explained via molecular orbital theory [47,72].

3.2. Activation of substrate molecules

The activation of substrate molecules on different types of metal species is directly associated with the metal-reactants interaction. When substrate molecules are adsorbed by metal species, there will occur orbital hybridization between adsorbed molecules and metal. In 2013, Sitja et al. studied the adsorption energy of CO molecules on Pd particles with different sizes (0.6–6 nm) [73], and found when the Pd particles size is larger than 1.8 nm, the adsorption energy of CO increases with the increase of the particle size. Whereas when the size of Pd particle is below 2 nm, the CO adsorption energy exhibits random change, which is owing to the atomicity variation derived from the change of electronic and geometric structures. These variations in the adsorption energy of CO suggest the metal species transform from nonmetallic to metallic when the particle size is changed from molecule-like state to bulk-like state.

When substrate molecules are adsorbed on metal species, the corresponding geometric distortion will also rely on the particle size. In 2014, Lei et al. investigated the structural changes when Pt nanoparticles of 1–3 nm interacted with substrate molecules [74], and found obvious relaxation of Pt-Pt bonds when adsorbing small molecules, which is the result of orbital hybridization between the molecules and metal species. Whereas this adsorbate-induced lattice relaxation becomes smaller when Pt nanoparticles size increases to 2–3 nm, which is owing to the lower numbers of under coordinated Pt atoms.

In addition, due to the interaction between substrate molecules and metal species, the metal species with different types may undergo dynamic changes under various treatments. Newton et al. dynamically observed the substrate molecule-induced size and shape changes of Pd nanoparticles [75]. Nagai et al. found the effective redispersion of Pt nanoparticles on creia-based oxide supports when treated with oxidative and reducing atmosphere [76]. Corma et al. also reported the reversible transformation of Pt nanoparticles into single Pt atoms through controlling temperature and atmosphere [77]. A thorough understanding of the interaction between substrate molecules and metal species can be useful to explain the catalytic performance of the supported metal catalysts.

4. Heterogeneous selective oxidation over supported metal nanoparticles and single atoms

4.1. Selective oxidation of methane

The activation and selective transformation of methane into liquid oxygenates is a captivating approach to lock carbons in transportable value-added chemicals [49,78,79]. In the present situation, the selectivity of the methane oxidation has to be further raised so as to decrease the formation of undesirable non-selective products, particularly CO_2 . Further optimizing the catalyst and the process is essential in the current chemical industry. However, the direct activation of CH_4 is extremely challenging for two reasons. On one hand, CH_4 only has saturated C-H bonds, whose bond dissociation energy is very high ($434.7 \text{ kJ} \cdot \text{mol}^{-1}$), thus a high energy barrier and severe conditions are necessary to realize the conversion of CH_4 . On the other hand, the products reactivity is usually much higher than that of CH_4 , thus they are easily over-oxidized to CO or CO_2 under reaction conditions [3,80]. In recent years, various heterogeneous catalysts have been developed for the direct oxidation of CH_4 to methanol, but according to the reported literatures, there was no assigned active site for this transformation, because multiple structures were verified to activate methane molecule [81,82].

After decades of research, Cu-zeolite prepared by ion exchange method is confirmed as the most promising catalyst at present. The conversion of CH_4 to methanol catalyzed by Cu-zeolite is shown in Fig. 3a [80]. First, the Cu-zeolite material is activated at high temperature in air or oxygen atmosphere, then cooled to 100–200 °C. At this time, the CH_4 molecules are adsorbed on the Cu species, and an O atom is inserted into the C-H bond. After a period of time, the adsorbed methanol is desorbed when water vapor is introduced. That is to say, the direct contact between CH_4 and oxygen is avoided in the above reaction, and the conversion of CH_4 to methanol is achieved through a stepwise reaction. The Cu-mordenite (MOR) catalysts with different Cu exchange amounts were reported [81], the authors found every two Al sites corresponds to three Cu^{2+} ions. Then the authors proposed a schematic diagram of the active site with the aid of in-situ x-ray absorption near edge structure (XANES) and extended x-ray absorption fine structure (EXAFS) (Fig. 3b,c). It can be seen that the $Cu_3O_3^{2+}$ clusters are located in the MOR channel and are stabilized by two Al acid sites, these trinuclear copper oxygen clusters exhibited much higher activity and selectivity for the oxidation of CH_4 to methanol. In this report, although a heterogeneous catalyst is employed, the conversion of CH_4 to methanol is indeed achieved through a multi-step reaction, which is significantly different from the conventional continuous fixed-bed reaction. Another report is that the authors simultaneously introduced CH_4 , oxygen and water into the fixed-bed reactor to achieve continuous oxidation of CH_4 to methanol (Fig. 3d) [82], no methanol is produced after less than ten hours

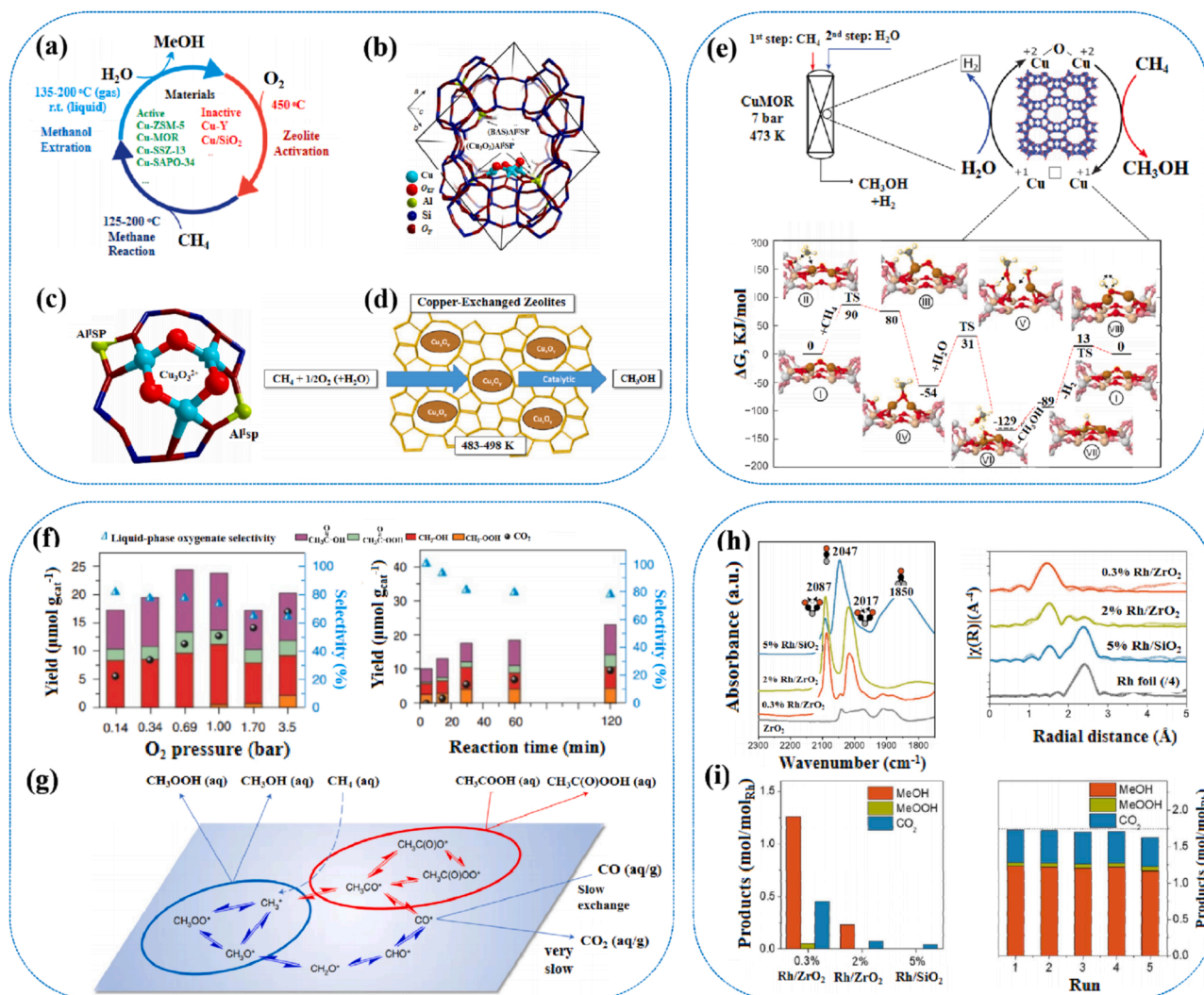


Fig. 3. (a) Illustration of the three-step conversion of methane to methanol including [80]. (b,c) Structure and location of $[\text{Cu}_3(\mu\text{-O})_3]^{2+}$ cluster in mordenite predicted by DFT [81]. (d) Catalytic oxidation of methane into methanol over copper-exchanged zeolites with oxygen at low temperature [82]. (e) The mechanism of the partial oxidation of methane using water as oxidant [83]. (f) The effect of O_2 partial pressure and reaction time on the catalytic performance of 0.5% Au-ZSM-5 catalysts for methane oxidation [87]. (h) DRIFT spectra of CO molecules adsorbed on various catalysts. Rh K edge k^3 -weighted Fourier transformed EXAFS spectra of various catalysts. (i) Direct methane oxidation results on various catalysts [88].

through conventional process (using H_2O to desorb the adsorbed methanol species).

In 2017, Bokhoven et al. reported an anaerobic method for the oxidation of CH_4 to methanol, which uses Cu-zeolite as catalyst and water as a soft oxidant, obtaining very high selectivity (~97 %) to methanol [83]. As shown in Fig. 3e, the C-H bond in methane is activated, and then the insertion of O atom is achieved. At the same time, the copper species of Cu(II) is reduced to Cu(I). Afterward, water vapor was introduced to achieve the desorption of methanol and the re-oxidation of Cu(I) to Cu(II). Moreover, the double Cu centers were confirmed to be the active species for this transformation through in-situ XANES, IR, and DFT calculations. Although much progress has been made on identifying the nature of active sites, the catalytic properties of Cu-zeolite is still far below the practical application requirements, thus the exploration of novel materials for the transformation of CH_4 to methanol is very

indispensable. Then Lercher et al. reported the oxidation of CH_4 to methanol catalyzed by Cu-oxo clusters stabilized in NU-1000 metal-organic framework (MOF) [84]. In this work, Cu species were supported on the NU-1000 by atomic layer deposition (ALD), and found Cu oxide clusters as an active site for catalyzing the oxidation of CH_4 to methanol

by means of in-situ EXAFS and XANES. However, it should be pointed out that the thermal stability of MOF supports is far less than that of zeolite, so the Cu/NU-1000 catalyst can only work at 150 °C rather than 200 °C like zeolites. In addition, CH_4 can undergo highly facile C-H bond cleavage on IrO_2 surface [85]. Rui et al. prepared bicomponent catalyst IrO_2/CuO cluster for the direct oxidation of CH_4 to methanol under mild conditions, IrO_2 was used for CH_4 activation and CuO for selective oxidation [86]. Furthermore, Hutchings et al. reported Au nanoparticles supported on the zeolite ZSM-5 was able to oxidize methane into methanol and acetic acid in water using O_2 at temperatures between 120 and 240 °C (Fig. 3f) [87]. Compared with the previously reported Cu-zeolite catalysts, for which only C1 products are formed, C2 oxygenates are the major products detected on Au-ZSM-5, indicating that the selective oxidation of methane over Au catalysts obeys a different mechanism (Fig. 3g), which mainly involves surface-bound intermediates instead of the species in the fluid phase.

Recently, SACs have attained ever increasing attention in heterogeneous catalysis owing to their high activity and selectivity. SACs with specific coordination metal centers on active supports exhibit remarkable reactivity and selectivity for CH_4 oxidation. Due to the electrostatic polarization of C-H bond, SACs can greatly reduce the activation energy

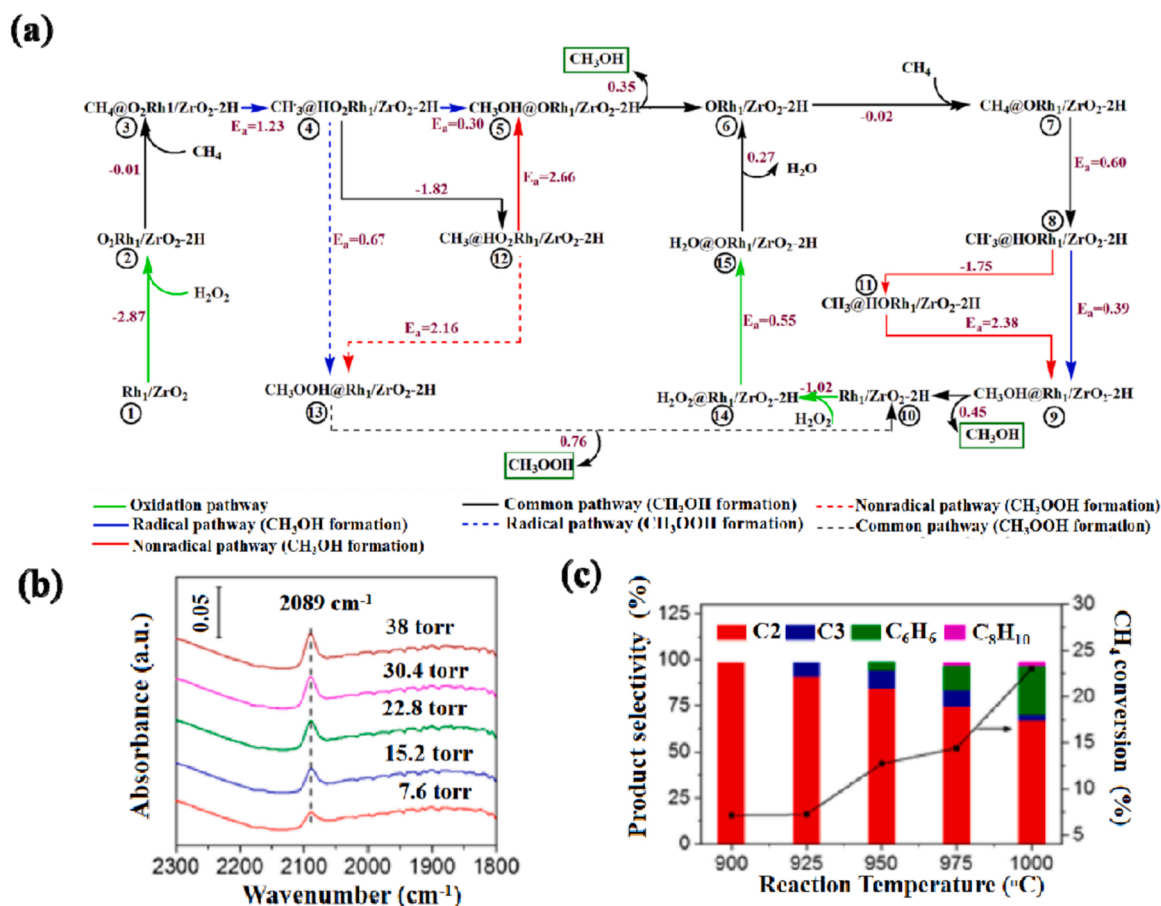
so as to accelerate the reaction rates at low reaction temperatures. The intermediate can be stabilized and the over-oxidation of reaction products can be prevented owing to the unique metal-support interaction [88]. In addition, For the selective oxidation of CH₄, once the first C-H bond of CH₄ is activated, the dissociation of the remaining C-H bonds on the metal surface will hamper the direct conversion of methane into chemicals. Guo et al. carried out experimental and theoretical work to confirm Cu₁-O₄ entity acting as active site can preferentially activate CH₄ instead of CH₃OH because of the entropic and solvation contribution [89]. Besides, the C-H bond of CH₄ can be easily activated by the distinct O-FeN₄-O structure formed in graphene, it follows the free radical pathway and the reaction energy barrier is only 0.79 eV [90]. Lee et al. reported ZrO₂ supported single-atom Rh (Rh₁/ZrO₂) catalyst for the activation of CH₄ [91]. The single atomic dispersion of Rh was verified via diffuse reflectance infrared Fourier transform (DRIFT) spectroscopy and EXAFS analysis (Fig. 3h). The property of Rh active sites could greatly affect the product distribution for CH₄ oxidation. The highest yield of methanol could be obtained over single atomic Rh catalyst, whereas Rh nanoparticles supported on SiO₂ could only produce CO₂. Furthermore, Rh single atom catalyst exhibited excellent recyclability, almost no decrease of the oxygenated products yield after being recycled five times is observed (Fig. 3i). DRIFTS measurement and DFT calculation indicated that the CH₃ intermediates could be stabilized on the Rh₁/ZrO₂ catalyst upon methane adsorption, and thus benefiting the formation of the desired product methanol.

The above transformation of CH₄ to methanol was achieved at a solid-gas interface in ZrO₂, while Hutchings et al. found the transformation rate of CH₄ to methanol at a solid-liquid interface is higher than that at a solid-gas interface [92,93]. Then Tao et al. explored the

conversion of CH₄ over Pd₁O₄ single atoms at a solid/liquid/gas interface and compared the thermodynamic behavior of the formation of methanol and methylperoxide [94]. Pd₁O₄ single-sites were supported on the internal surface of the microporous silicate, which showed high CH₄ conversion and 86.4% methanol selectivity in aqueous phase conditions, H₂O₂ was used as oxidant. It is worth noting that the extra H₂O₂ in the reaction system could oxidize methanol into formic acid, so they added CuO into the catalyst to dissociate the extra H₂O₂, thus preventing the further oxidation of methanol to formic acid, and enhancing the selectivity of methanol. Moreover, they found that the reaction toward methanol production over Pd₁O₄ single atoms was thermodynamically favorable compared to the formation of methylperoxide byproduct. Later, Li et al. carried out first-principles calculations to investigate the catalytic mechanisms for methane oxidation on Rh₁/ZrO₂ using H₂O₂ as oxidant (Fig. 4a) [95]. Interestingly, they found H₂O₂ could undergo dissociative

adsorption on Rh₁/ZrO₂ spontaneously, which is quite different from the other experimentally explored ZrO₂ supported Pd, Ir and Pt SACs, so that the active site was initiated and the surrounding oxide support surface was hydrogenated. This hydrogenation process of the oxide support surface suppressed the further oxidation of methanol into formic acid and CO₂.

As is known to all, Pt is efficient in the activation of C-H bond in hydrocarbons [96,97], however, the traditional catalysts such as Pt nanoparticles or clusters tend to accumulate carbon at high temperatures, so the application of Pt-based catalyst in the transformation of CH₄ is limited. While the conversion of CH₄ into these hydrocarbons are of great significance [98–100]. In 2018, Wang et al. reported nanoceria supported single-atom platinum delivered remarkable coking resistance



for direct conversion of CH₄ into light hydrocarbons [101]. DRIFTS analysis of CO adsorption and HAADF-STEM characterizations were used to confirm the atomically dispersion of Pt (Fig. 4b). The conversion of CH₄ over Pt₁@CeO₂ catalyst with 0.5 %–1 % loading of Pt could reach 12 %, and the total selectivity toward hydrocarbons were over 95 % (Fig. 4c), which were much higher than those of their nanoparticulated counterpart. Moreover, both the high catalytic activity and selectivity of Pt₁@CeO₂ were well maintained after 40 h of continuous reaction at 975 °C, suggesting the developed single atom catalysts possess the ability to suppress carbon coking during the direct conversion of CH₄. Besides, a few SACs such as Rh₁-graphene/Ni and Fe₁/MoS₂ have been proposed as potential catalysts for CH₄ selective oxidation into methanol theoretically [102,103]. In a word, SACs provide the possibility to activate CH₄ under mild reaction conditions. The selective oxidation of methane over representative catalysts are summarized in Table 1.

Besides, photocatalytic oxidation of CH₄ is an alternative approach to enable this difficult reaction to occur at mild temperatures [111]. Chen et al. found when the particles size of zinc oxide as reduced to nanoscale, it showed excellent activity for methane oxidation under sunlight illumination [112], the addition of nano silver enhanced the photo-activity due to the surface plasma resonance. Quantum-sized bismuth vanadate nanoparticles also exhibited superior photocatalytic activity and high methanol selectivity with water as solvent [113]. Atomic-scale metals working as active center have also been considerably applied for photocatalysis. Among, atomically dispersed gold species demonstrate a specific tip-enhanced local electrons field, and contributes the activation of methane and formation of methanol [114]. Combined experimental and DFT calculations confirms that isolated Cu atoms stabilized by four oxygen moieties on ZSM-5 as active site can preferentially activate methane instead of methanol [115]. Moreover, the types of reactive oxygen species play an important role in the products selectivity, which was determined by the band structure [116].

4.2. Aerobic selective oxidation of alcohols

The selective oxidation of alcohols to corresponding aldehydes or ketones is an important reaction in industry and academia [117,118], because aldehydes and ketones are indispensable intermediates or precursors for the production of fine and specialty chemicals. Over the past few years, numerous work on the utilization of metal nanoparticles for the selective oxidation of alcohol has been carried out [119–121]. There are three essential steps in the oxidation of alcohols over noble metals

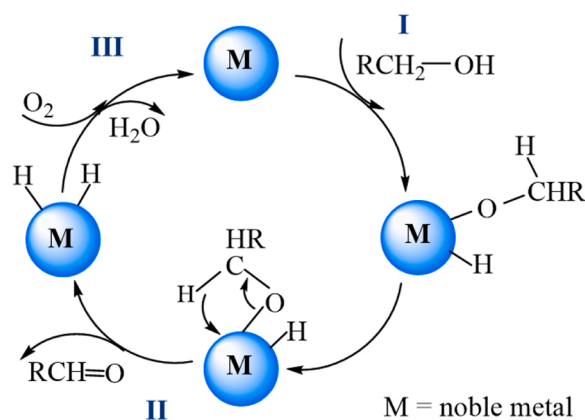


Fig. 5. Oxidation of alcohol to the corresponding aldehyde over a noble metal.

(Fig. 5). The first step is the insertion of a metal atom into the O–H bond of alcohol, forming a metal alkoxide and a metal hydride. The second step is the removal of a hydrogen by the noble metal through the elimination process of β -hydride, obtaining aldehyde or ketone. And the third step is the regeneration of noble metal active sites [3].

The catalytic performances of metal nanoparticles can be influenced by many factors, including the size [119,122] and shape [123,124] of metal clusters and nanoparticles, promoters [125], interactions between supports and active sites [117], and so on. Next, the size effect of metal nanoparticles on their catalytic performance for the oxidation of alcohols was illustrated. As shown in Fig. 6a, different sizes of Pd particles over SiO₂-Al₂O₃ support were prepared via regulating the Si/Al ratio. Pd nanoparticles supported on three different types of supports exhibited similar variation on size-dependent turn-over frequency (TOF) for benzyl alcohol oxidation, and it showed a maximized activity at a medium mean size (3.6–4.3 nm), indicating this is a structure-sensitive reaction. The ratio of surface terrace Pd atoms to coordinatively unsaturated Pd atoms is corresponded to 2.3–3.1, this conformation of Pd active sites contributes to the adsorption of reactant and the activation of β -hydride [122]. Hydrotalcite-supported Au nanoparticles with different sizes (ranging from 2.1 to 21 nm) were also prepared for the oxidation of benzyl alcohol oxidation, it can be seen from Fig. 6b, both TOF and initial rate increase with decreasing the size of Au nanoparticles. Specially, the TOF increases dramatically when the particle size of Au decreases from \sim 4 nm, indicating these coordinatively unsaturated surface Au atoms are active for the activation of C–H bond in alcohol molecules [119].

Except for the size of metal clusters and nanoparticles, the shape of particle also has an significant impact on their catalytic performances, and relative effects have been investigated with Pt nanoparticles for the oxidation of alcohol [123–125]. Cuenya et al. reported four different shapes of Pt nanoparticles supported on γ -Al₂O₃ for the oxidation of 2-propanol [126]. These nanoparticles shapes of Pt NP/ γ -Al₂O₃ samples were obtained based on the fitting of EXAFS data and the measured TEM diameter (Fig. 6c), and they exhibited different activities for 2-propanol oxidation (Fig. 6d), implying the shape of the nanoparticles has important influence on its catalytic performance. Among the investigated catalysts, the Pt nanoparticles possessing bilayer structure demonstrated the highest catalytic activity for the oxidation of 2-propanol, this bilayer structure enlarged the contact area between Pt and γ -Al₂O₃ support, thus facilitating the oxidation reaction. Moreover, the onset reaction temperature of 2-butanol oxidation was largely depended on the shape of Pt nanoparticles [127]. The Pt nanoparticles with more edges and corners were found to be more selective for the desired product 4-butanone, and less selective for the combustion product CO₂.

The catalytic property of a mono-metallic catalyst can be greatly enhanced by adding promoters. For the oxidation of benzyl alcohol, compared with the unmodified Pt/CNT, the addition of FeO_x promotes

Table 1

The selective oxidation of methane to methanol over various catalysts.

Catalyst	T (°C)	P (bar)	Sel. (%)	Yield ($\mu\text{mol}\cdot\text{g}^{-1}$)	Ref.
Supported nanoparticles/clusters					
Cu ₂ O ₂ -Mordenite	175	-	-	-	[104] J. Am. Chem. Soc. 2005
Cu-Mordenite	200	-	-	15	[105] Nature 2016
Cu-Mordenite	200	7	97	0.2	[83] Science 2017
Cu-NU-1000	150	-	45	17.7	[84] J. Am. Chem. Soc. 2017
IrO ₂ /CuO	150	20	-	1937	[86] ACS Energy Lett. 2019
CeO _x /Cu ₂ O	177	-	-	1	[106] J. Am. Chem. Soc. 2016
CeO ₂ -Cu ₂ O	-	-	92	-	[107] Science 2020
Supported single atoms					
Rh ₁ /ZrO ₂	260	-	-	1.25	(95) ACS Catal. 2019
Pd ₁ O ₄ @ZSM-5	-	-	86	2.72	(94) Angew. Chem. Int. Ed. 2016
Cr ₁ /TiO ₂	50	30	93	1.13×10^6	(108) Angew. Chem. 2020
Rh ₁ /CeO ₂	50	5	94	1.32×10^6	(109) Nat. Commun. 2020
Cu ²⁺ -Rh ₁ /TiO ₂	150	31	99	5200	(110) Angew. Chem. 2022

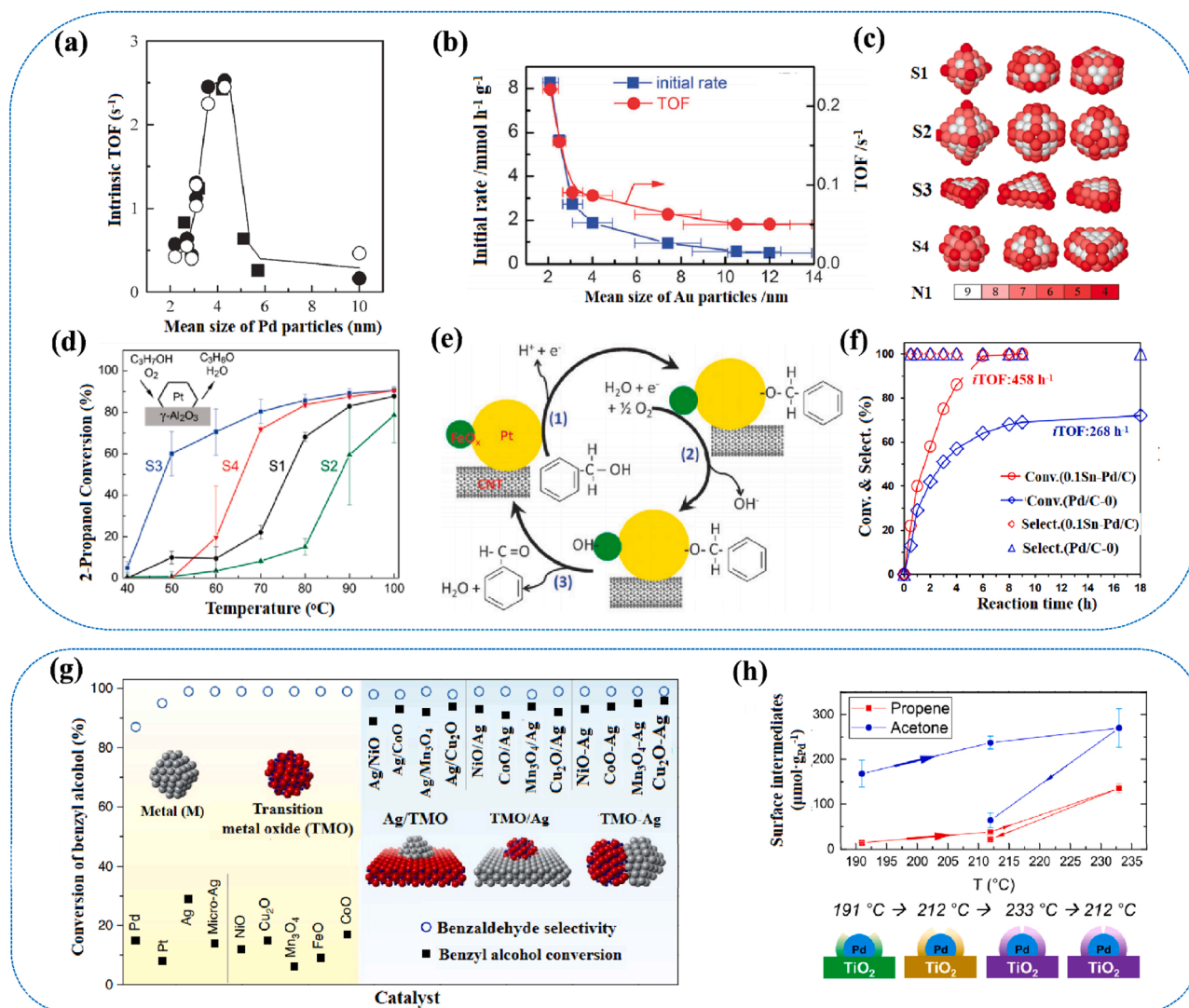


Fig. 6. (a) Dependence of the intrinsic turnover frequency on the mean size of Pd particles [123]. (b) Size dependence in hydrotalcite supported Au nanoparticle-catalyzed transformation of benzyl alcohol [119]. (c) Models of different Pt nanoparticles with similar particle size but different geometric shapes [78]. (d) Conversion of 2-propanol during oxidation reactions [126]. (e) Reaction scheme for the selective oxidation of benzyl alcohol to benzaldehyde over a FeO_x/Pt/CNT catalyst [125]. (f) Time course curves on the Pd/C-0 and 0.1Sn-Pd/C catalysts for base-free aerobic oxidation of alcohol to corresponding aldehyde [128]. (g) Conversion of benzyl alcohol (solid square) and selectivity to benzaldehyde (hollow circle) over metal nanoparticles, TMO nanoparticles, nano-Ag/micro-TMO, nano-TMO/micro-Ag and Ag-TMO nanocomposites [130]. (h) Surface intermediates measured via SSITKA (surface intermediates = rate (mol·min⁻¹·g_{Pd}⁻¹)/TOF (min⁻¹)); Sketch of SMSIs. The arrows in the lines connecting the data signal the sequence in the change of temperature: 191 °C → 212 °C → 233 °C → 212 °C [131].

the activation of reactant benzyl alcohol and molecule oxygen (Fig. 6e), the formed Fe-OH_{ads} removes the dissociated hydrogen from α-C of benzyl alcohol, thus releasing the desired product benzaldehyde, the promoting effect of FeO_x was owing to the suppressed adsorption of by-products [125]. As shown in Fig. 6f, the addition of Sn promoter can dramatically increase the transformation of alcohol over Pd/C-0 catalyst, 100 % aldehyde yield can be achieved after 6h, nevertheless the yield of aldehyde can only reach 70 % after 18 h of reaction in absence of Sn [128]. The Sn⁴⁺ ions in SnO₂ as electronic promoter can increase the interfacial electron density of Pd atoms in Pd/C, and thus improving the adsorption and activation of reactants. Moreover, the Sn promoter can also enhance the interaction between Pd and carbon support, thus Sn-Pd/C catalyst possesses high catalytic stability. Besides, the addition of promoter can modify the properties metal-O bonds, and thus improving their catalytic performances [129].

The support effect derived from the interactions between active sites and supports can also greatly affect the catalytic performance of a

catalyst via modifying the physico-chemical properties of active sites. Li et al. reported a variety of metal/oxide combinations were highly active and selective for the selective oxidation of benzyl alcohol and other primary alcohols [130]. Three different types of Ag/TMO (TMO refers transition metal oxide) interfaces were prepared, including Ag-TMO nanocomposite, nano-Ag supported on micro-TMO, and nano-TMO supported on micro-Ag. As shown in Fig. 6g, Ag-Cu₂O shows much better catalytic performance for the conversion of benzyl alcohol than that of pure nano-Ag and nano-Cu₂O. Even the performances of the physically mixed nano-Ag and other nano-TMO (NiO, CoO, and Mn₃O₄) are much higher than that of the pure nano-Ag or nanoTMO. The formed interfacial sites between Ag and TMO contributes the dissociation of O₂, thus facilitating the adsorption of benzyl alcohol and the cleavage of O-H bond. In addition, alcohols can be used as reducing agents to reduce metal oxides. The strong metal-support interaction can be generated during the conversion of alcohols, which can be verified through the steady-state isotopic transient kinetic analysis (SSITKA) (Fig. 6h) [131].

And Corma et al. reported gold nanoparticles could interact with the nanometric ceria surface, the positive oxidation states of gold can be stabilized via creating Ce^{3+} and oxygen-deficient sites in the ceria [117]. Besides, MOF-supported nanoparticles, as an emerging class of porous materials, exhibit unexpected catalytic performance for the selective oxidation of alcohols [132,133].

As described before, metal nanoparticles exhibit remarkable catalytic performance for the selective oxidation of alcohols. In recent years, SACs have been reported to be efficient for the transformation of alcohols. In 2007, Lee et al. developed mesoporous alumina-supported palladium catalysts for the oxidation of allylic alcohols [134]. Fig. 7a shows that considerable bright spots are distributed on the mesoporous alumina.

support. The TOF of Pd species in the oxidation of crotyl alcohol is highly dependent on the size of Pd (Fig. 7b). When the Pd size increases from single-site to clusters and to nanoparticles, its corresponding TOF decreases dramatically. And Pd SACs possess the maximized TOF value and high selectivity for butenal. Compared with Au nanoparticle catalysts, Au_1/CeO_2 demonstrated much higher activity and selectivity for the selective oxidation of alcohols, which can be ascribed to the maximized interfacial sites between Au single atom and CeO_2 supports, and thus favoring the activation of lattice oxygen. Besides, the developed Au_1/CeO_2 catalyst showed excellent stability and operability in alcohols oxidation (Fig. 7c) [135]. In addition, various non-noble metal catalysts have been exploited for substituting noble metals in heterogeneous catalysis. Single cobalt atoms embedded in nitrogen-doped graphene (SACo@NG) was demonstrated as the main active sites for the selective oxidation of benzyl alcohol by peroxydisulfate via both radical and non-radical pathways [136]. Both the conversion of benzyl alcohol and the selectivity of benzaldehyde over SACo@NG were more than 90 %, and the recycling test showed SACo@NG possessed excellent stability after four runs, which is owing to the stably bonded Co atoms with N.

Moreover, defect-containing MoS_2 confined iron atoms (FeSA/MoS_2) delivered superior catalytic performance in the selective oxidation of benzyl alcohol into benzaldehyde, with almost 100 % conversion and 99 % selectivity (Fig. 7d). The TOF reached 2105 h^{-1} , which is far superior than that of Fe NPs/ MoS_2 , $\text{Fe}_1/\text{N-C}$, hemin, iron(II) phthalocyanine, Pt/C and FeCl_3 (Fig. 7e). In addition, the excellent conversion and selectivity were well maintained after reaction 16 h. DFT calculations indicated $\text{Fe}_1\text{-S}_3$ moieties acted as active sites so as to significantly reduce the energy barriers [137].

The selective oxidation of alcohols can also be catalyzed by atomically defined undercoordinated copper atoms over nitrogen-doped carbon ($\text{Cu}_1/\text{N-C}$) under mild conditions, giving high conversion of cinnamyl alcohol and 99% selectivity of cinnamaldehyde [138]. The apparent activation energies of $\text{Cu}_1/\text{N-C}$ were calculated to be $37.5 \text{ kJ}\cdot\text{mol}^{-1}$, which is about half of the corresponding Cu NPs/ N-C (Fig. 7f), implying the higher intrinsic activity of $\text{Cu}_1/\text{N-C}$ in the transformation of this reaction. XAFS measurements and DFT calculations confirm Cu species in $\text{Cu}_1/\text{N-C}$ were in the oxidized state and one Cu atom coordinated with 4 surrounding N atoms, this unique coordination environment favored the activation of reactant and the desorption of the desired product. The selective oxidation of alcohols over various catalysts are summarized in Table 2. In-depth understanding the catalytic mechanism in these non-noble metal system via in-situ spectroscopic experiment or isotopic studies is urgently needed to further improve their performance and stability.

In addition, there are also considerable studies on the development of supported nanoparticles and SACs for photocatalytic selective oxidation of alcohols. The visible-light harvesting, electron-transport and charge-separation of amine modified MOF will be improved when doped with Ni nanoparticles, resulting in enhanced photocatalytic activity [140]. The dopant P into carbon nitride can also greatly improve the selectivity of photocatalytic oxidation alcohol into aldehyde, which

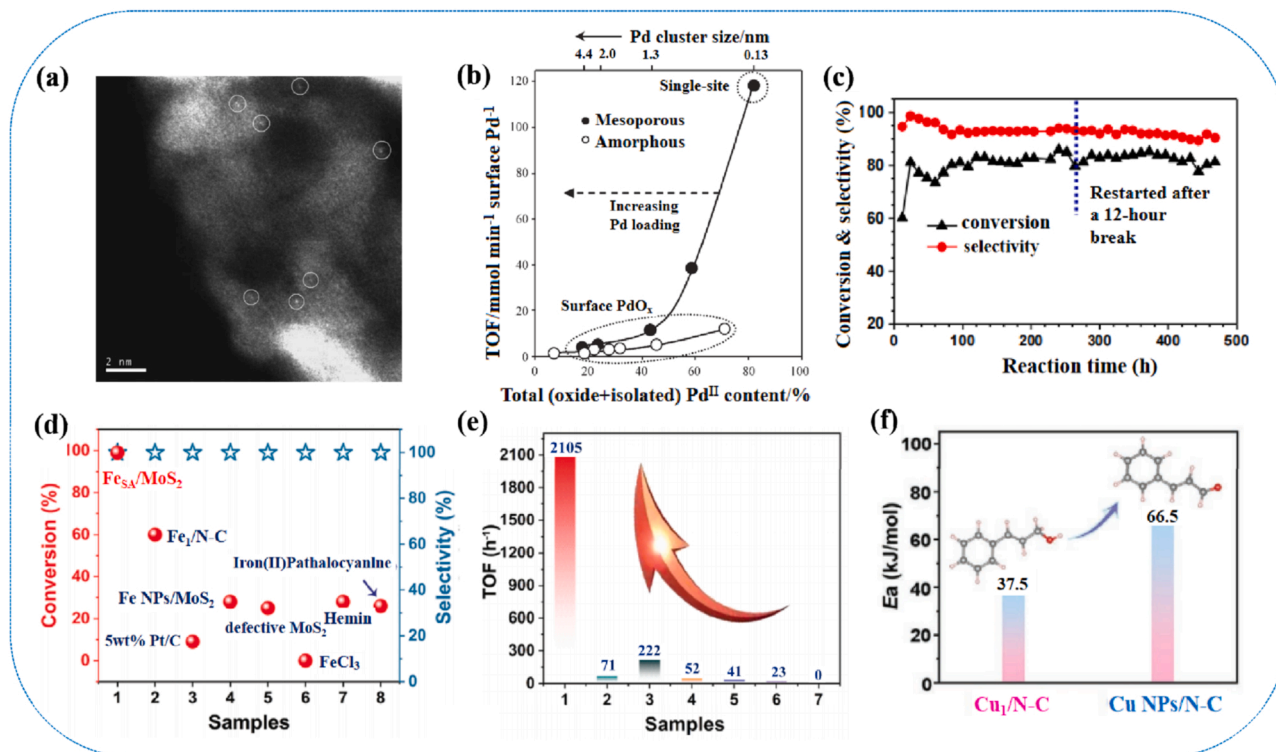


Fig. 7. (a) HAADF STEM image of a 0.03 wt% Pd/meso- Al_2O_3 sample. (b) Catalytic performance of Pd clusters dispersed across conventional versus mesoporous alumina supports as a function of size and oxidation state in aerobic crotyl alcohol oxidation [134]. (c) Conversion and selectivity of benzyl alcohol oxidation over Au_1/CeO_2 catalyst in long-term test [135]. (d) Conversion and selectivity of samples for the selective oxidation of benzyl alcohol into benzaldehyde [137]. (e) TOF values (1: FeSA/MoS_2 ; 2: $\text{Fe NPs}/\text{MoS}_2$; 3: $\text{Fe}_1/\text{N-C}$; 4: hemin; 5: iron(II) phthalocyanine; 6: 5 wt% Pt/C; 7: FeCl_3) [80]. (f) The corresponding E_a values for the oxidation of cinnamyl alcohol to cinnamaldehyde over $\text{Cu}_1/\text{N-C}$ and Cu NPs/ N-C [138].

Table 2

The selective oxidation of various alcohols over different catalysts.

Reaction	Catalyst	T (°C)	P (bar)	Sel. (%)	Yield ($\mu\text{mol}\cdot\text{g}^{-1}$)	Ref.
Supported nanoparticles/clusters						
	Pd NPs/SiO ₂ -Al ₂ O ₃	79	-	99	-	[121] <i>Green Chem.</i> 2013
	Au NPs/Hydrotalcite	120	-	-	-	[119] <i>Chem. Commun.</i> 2011
	Pt NPs/ γ -Al ₂ O ₃	90	-	-	-	[126] <i>J. Am. Chem. Soc.</i> 2010
	Pt NPs-FeO _x /CNT	75	-	100	-	[125] <i>Chem. Commun.</i> 2011
	Pd NPs-Sn/C	120	3	100	-	[127] <i>ACS Catal.</i> 2020
	K-MnO ₂ / γ -Al ₂ O ₃	100	-	99	-	[128] <i>J. Mol. Catal. A: Chem.</i> 2009
	Pd NPs/TiO ₂	191	-	100	2750	[131] <i>ACS Catal.</i> 2021
Supported single atoms						
	Pd ₁ /meso-Al ₂ O ₃	60	-	91	29900	[134] <i>Angew. Chem. Int. Ed.</i> 2007
	Au ₁ /CeO ₂	150	10	98	-	[135] <i>Angew. Chem. Int. Ed.</i> 2018
	Co ₁ /N-Graphene	50	-	90	-	[136] <i>Small</i> 2021
	Fe ₁ /MoS ₂	120	-	99	-	[137] <i>Small</i> 2022
	Co ₁ /N-C	100	-	99	-	[138] <i>Small</i> 2022
	Pd ₁ /CeO ₂	100	1	100	-	[139] <i>Angew. Chem.</i> 2022

is due to the reduced the oxidant ability of carbon nitride [141]. The insertion of single Co atom into porous organic cage framework can significantly decrease the charge transfer resistance, inhibit the electron/hole recombination, and broaden the light absorption, thus considerably enhancing the photocatalytic performance [142]. Moreover, the incorporation of Co atoms into peroxydisulfate can act as active sites for the activation of benzyl alcohol via both radical and non-radical pathways [143].

4.3. Epoxidation of alkenes

The epoxidation of alkenes into corresponding epoxides is an important industrial process, as epoxides are important intermediates in fine chemical and pharmaceutical industries [144,145]. Although traditional homogeneous catalytic systems involving in this transformation exhibit excellent performance, they usually employ H₂O₂ or organic hydroperoxides as oxidizing agents, and expensive approaches are needed for product separation and catalyst recovery. Whereas heterogeneous catalysts possess several advantages for epoxidation reactions, including mild reaction conditions, ease of product separation and catalyst recyclability. Silver-based catalysts were identified as the most efficient for the epoxidation of ethylene and propylene [146–148], other catalytic systems such as Au supported metal oxides [149], Cu (111) [150], Ti-MCM-4 [151], WO₃ [152], molybdenum-based catalysts [153] were highly efficient for the epoxidation of bulky alkenes.

The epoxidation of ethylene to value-added ethylene oxide (EO) is one of the most important industrial processes, as EO is an indispensable chemical intermediate which can be further converted to major chemicals such as pharmaceuticals, detergents, plastics, and antifreeze. According to the Global Economic Analysis report, the worldwide production of EO was over 34.5 million tons in 2016 [154]. EO is industrially produced by gas-phase selective oxidation of ethylene with supported Ag/Al₂O₃ catalysts in fixed-bed tubular reactors [155–158].

The selectivity of EO is the most important parameter, which determines the performance of an EO catalyst. For an unpromoted silver catalyst, its EO selectivity only approaches 50 % [159], while the EO selectivity can achieve over 90 % with the addition of promoters such as Cs, Re, Mo, or the inhibitor CH₂Cl₂ [160]. And the catalytic selectivity for ethylene epoxidation on Ag/Al₂O₃ catalysts largely depends on the geometric structures of Ag nanoparticles, the type of active oxygen species, and reaction conditions.

Linic et al. compared the catalytic performance of Ag nanowires, nanocubes, and spherical with different sizes [161]. Both the shape and size of Ag particles can affect EO selectivity (Fig. 8a). The discrepancy in the selectivity of EO can be ascribed to their different exposed facet of Ag. The surfaces of Ag nanocubes and nanowires.

possess higher concentrations Ag(100) facet, which prefers the ring closure of the surface oxametallacycle, and thus producing the desired product EO. While the Ag spherical particles are dominated by the Ag (111) facet, which always lead the over-oxidation of EO. For a given Ag particle shape, the effect of particle size on EO selectivity is owing to the concentration of undercoordinated surface sites. The smaller particles possess higher undercoordinated sites concentrations, and thus the catalysts are less selective. Hellman et al. also verified Ag particles with Ag(100) facet contributed to the activation of ethylene and the formation of EO (Fig. 8b) [147]. Besides, the silver lattice and defect sites can undergo reconstruction to create pores under reaction conditions, the vinyl chloride can suppress the formation of void and redisperse silver particles [146].

The nature of oxygen species adsorbed on the silver surface during the oxidation of ethylene has an important influence on the reaction path. The generally accepted idea is that the nucleophilic oxygen is usually involved in the complete oxidation of ethylene to CO₂, while the electrophilic oxygen can participate in the production of EO. Carbonio et al. utilized in-situ UHV X-ray Photoelectron Spectroscopy (XPS) to investigate the interaction between oxygen and a silver surface, they

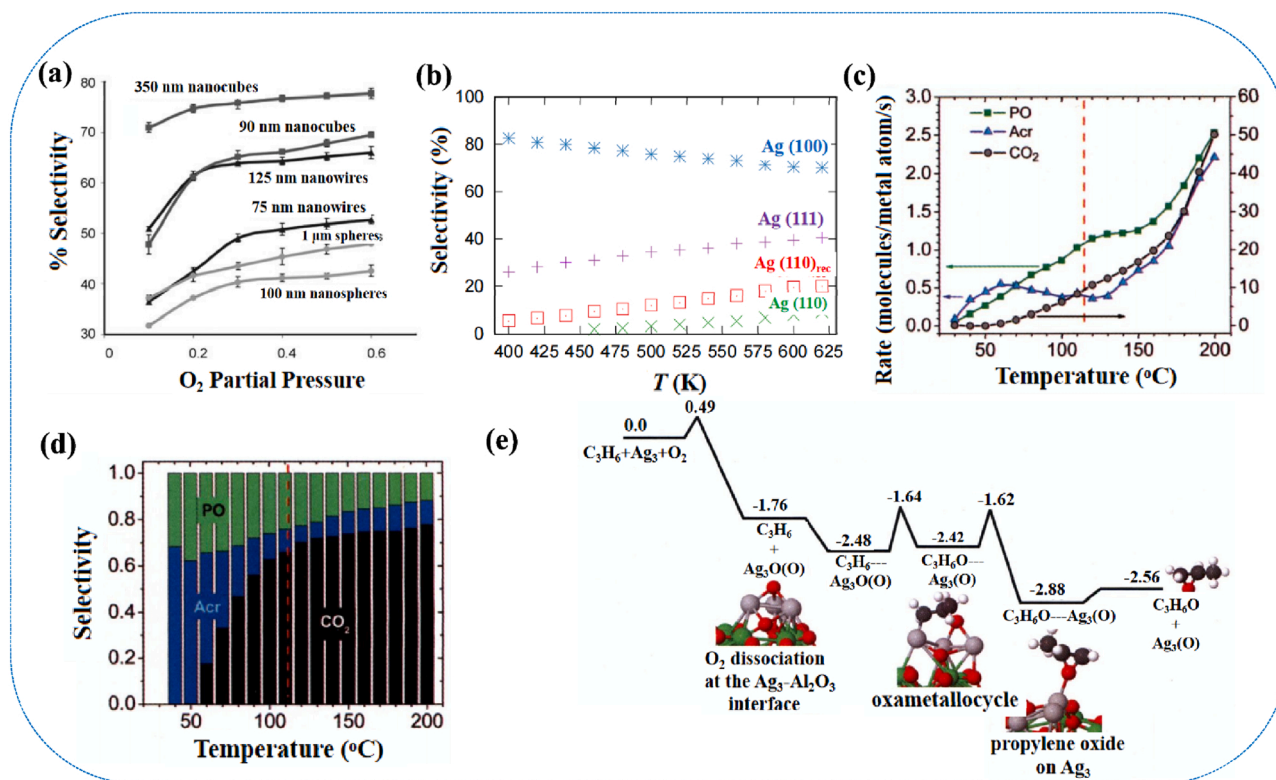


Fig. 8. (a) Selectivity to EO for Ag nanocubes, nanowires, and nanospheres of different edge lengths and diameters. $T = 510$ K [161]. (b) Selectivity in the epoxide production as a function of temperature [147]. (c) Rate of propylene oxidation toward PO, acrolein (Acr), and CO₂ per surface silver atom. (d) Selectivity of propylene oxide, acrolein, and CO₂ versus temperature over Ag₃O clusters/Al₂O₃. (e) Reaction mechanism of oxidation of propene to propene oxide catalyzed by Ag₃O clusters based on DFT calculation [148].

found at least two different species, covalent oxygen-electrophilic oxygen (O_{elec}) and unreconstructed atomic oxygen participated in the epoxidation of ethylene [162]. Jones et al. reported the coadsorbed oxygen could induce the reconstruction of catalyst surface, resulting in a local competition with the adsorbed Ag atoms, partially lifts the Ag/O reconstruction. The resulting catalyst surface possessed the spectroscopic properties of O_{elec} , favoring the production of EO [163]. Bukhtiyarov et al. carried out in-situ O K-edge XAS to reveal O_{elec} was active in ethylene epoxidation, and there was no XAS features of molecular oxygen, indicating the origin of O_{elec} was atomic oxygen. Besides, the subsurface oxygen could increase the reactivity of Ag surface via inducing an upshift of its d -band center [164].

Propene oxide (PO) as raw material has been largely-scaled used in the polymer industry. PO is industrially produced by two-staged processes, including chlorohydrin process and Halcon (hydroperoxide) process [165]. In 1983, Taramasso first reported the synthesis of titanium silicalite (TS-1), which has high activity and selectivity for the epoxidation of olefins, the partial oxidation of cycloalkanes, the hydroxylation of phenol and the ammoxidation of cyclohexanone [166]. In 1991, Clerici et al. found that the selectivity of propylene epoxidation to PO on TS-1 using H₂O₂ could reach 94 %. Once this work was reported, researches related to propylene epoxidation on TS-1 catalyst continued to emerge [167]. The use of TS-1 for the epoxidation of propylene, in which the Ti(IV) sites possess a well-defined chemical environment, is a landmark in industrial alkene epoxidation. In 1998, Hayashi et al. found propene could be epoxidized over Au/TiO₂ in the gas-phase using O₂ and H₂, then the catalytic behaviors of Au/TiO₂ and related systems have aroused great concern from chemical industries as well as academia [168].

There are four important factors for preparing efficient Au catalysts in propene epoxidation. The first one is preparation method. Impregnation and chemical vapor deposition methods could not obtain

selective catalysts, whereas the deposition-precipitation method could result in selective oxidation [169]. The second one is support. Among single metal oxides, only anatase TiO₂ supported Au is selective for the production of PO at temperatures below 373 K. While when Ti-SiO₂ support is used, Au is selective to epoxidation under 473 K, with about 5 % conversion and more than 90 % PO selectivity [170,171]. The difference in Au-support interactions results in different capacities of substrates adsorption and products desorption, and thus affecting the activity and selectivity of supported Au catalysts. The third important factor is the size of Au particles [172], in which the size of Au particle ranging from 1.4 to 5.0 nm possesses increased amount of Au^{δ-}-Ti⁴⁺, and thus obtaining high propene conversion and PO selectivity. When the Au particle size increases to 7.0 nm, the large Au particles was dominant with Au^{δ+}, which contributes the deep oxidation of adsorbed PO. The fourth one is the additives. It has been reported that alkaline and alkaline earth salts might play an important role in the selective and epoxidation reactions [173], whereas the intrinsic mechanism of these promoters needs to be further understood. Moreover, the reaction atmosphere is also an important factor affecting the catalytic properties of propene epoxidation, the addition of H₂ into the mixed feed gas can promote the hydrogenation of O₂ to OOH, which is a feasible pathway for propene epoxidation in the aspects of both kinetic and thermodynamic viewpoints [174].

Apart from Au clusters, subnanometric Ag clusters are also active for epoxidation of propene. Vajda et al. reported that Ag₃/Al₂O₃ were efficient catalysts for propene epoxidation at low temperature [148]. It can be seen from Fig. 8c, propene could be readily transformed into PO and acrolein at 60 °C, which is quite different from the traditional Ag-based catalyst. Higher PO/acrolein ratios could be obtained when the temperature ranged from 70 to 100 °C (Fig. 8d). Theoretical calculations indicate that the O₂ molecules can be activated at the Ag₃/Al₂O₃ interface with a barrier of 0.49 eV (Fig. 8e), which is much lower than

the barrier of 1.19 eV on Ag(111) surface. And the net spin density on the Ag and O in the alumina-supported Ag_3O cluster is about 0.6, which can account for the extremely high catalytic activity and selectivity of silver trimers. By contrast, no spin density is present when atomic oxygen is adsorbed on the surface of Ag(111).

In addition, the electronic interaction between metal particles and support is crucial for the epoxidation of bulky alkenes. In this sense, Suib et al. observed the electronic perturbation at the Au-carbon interface, the doping of nitrogen into carbon enriches the surface charge density of Au sites [175]. The binding behavior of C=C bonds of styrene with catalytic centers is changed by the Au-carbon interaction, and thus resulting in a solvent-polarity-dependent selectivity. Co doped SnO_2 microspheres were reported as an efficient catalyst for the epoxidation of styrene under mild reaction conditions [176]. Introducing a small amount of Co dopant into SnO_2 can manipulate the electronic structure of SnO_2 , decrease the formation of oxygen vacancy, modulate the valence state of Sn, and thus adjusting the Sn-O interactions, which contributes the activation and coordination of styrene. In addition, the epoxidation of alkenes by molecular oxygen (air) can also be achieved at room temperature under visible light irradiation [177].

Recently, SACs have also shown great potential in the epoxidation of alkenes [178]. Han et al. investigated the possibility of Au atoms stabilized by defects on graphene for the epoxidation of ethylene via first-principles calculations [179], and found the.

interactions between Au atoms and graphene can tune the energy level of Au-d states (Fig. 9a), which accelerate the activation of O_2 and ethylene, and thus promoting the formation and dissociation of the intermediate peroxametallacycle. Moreover, the desorption of EO can be greatly facilitated when the coadsorbing O_2 and ethylene for initiating a new reaction cycle. These calculations indicate it is a helpful method to limit the coordination and interactions between active centers and reaction intermediates for the structure-sensitive reactions, and thus enhancing their catalytic selectivity. Su et al. also carried out DFT

calculations to study the epoxidation of alkene over M_1/POM SACs ($\text{M} = \text{Cu}, \text{Zn}, \text{Ag}, \text{and Au}$; $\text{POM} = [\text{PW}_{12}\text{O}_{40}]^{3-}$ [180], and found the dioxygen molecule can be activated by Zn_1/POM into O_2^- radical, forming the configuration of $[\text{POM}^{4-} \cdot \text{Zn}^{2+} \cdot \text{O}_2^-]^{3-}$. Then the complex interacted with the first ethylene molecule to form an EO molecule and a $[\text{Zn}]\text{O}$ complex. In step 3, the $[\text{Zn}]\text{O}$ complex interacted with the second ethylene molecule to generate another EO molecule. And the energy profile of the epoxidation of ethylene was obtained based on the M06L/6-31 G(d) calculations (Fig. 9b). The establishment of a catalytic cycle (O_2 and EO molecules acting as reactants, EO is the product) favors the process for ethylene epoxidation. In this catalytic reaction system, the adsorbed single Zn atom works as the active center, and the POM cluster support is utilized to stabilize Zn atom and accept electron. In general, this catalytic cycle has moderate energy barriers, indicating the explored Zn_1/POM SAC is potential for the epoxidation of alkenes.

Then Lei et al. reported single-site titanium on SiO_2 supported Au catalyst could achieve the transformation of propylene into PO [181], and found single-site titanium on metal oxide supports contributed to the high reactivity and selectivity in the epoxidation of propylene. High temperature calcination was used as an effective post-treatment method to control the titania structure and Ti-O coordination number, and thus improving the selectivity of PO from 54 % to 85 % (Fig. 9c). They found the PO selectivity was linearly correlated to the Ti-O coordination number in the Ti- SiO_2 support in the epoxidation of propylene on Au-based catalysts (Fig. 9d). That is, 4-fold coordinated single-site Ti favored the formation of PO, while the 6-fold coordinated single-site Ti preferred forming the undesired byproducts (propanal and CO_2). These conclusions are also confirmed in other studies [182–184].

Developing efficient heterogeneous catalysts for the epoxidation of styrene possesses high industrial and academic value. In 2020, Yang et al. reported the styrene epoxidation over single-atom Ru supported on microporous Beta zeolite catalyst [185]. The oxidation state of Ru in Ru_1/Beta was analyzed via XPS technique, the peak positions of Ru 3d

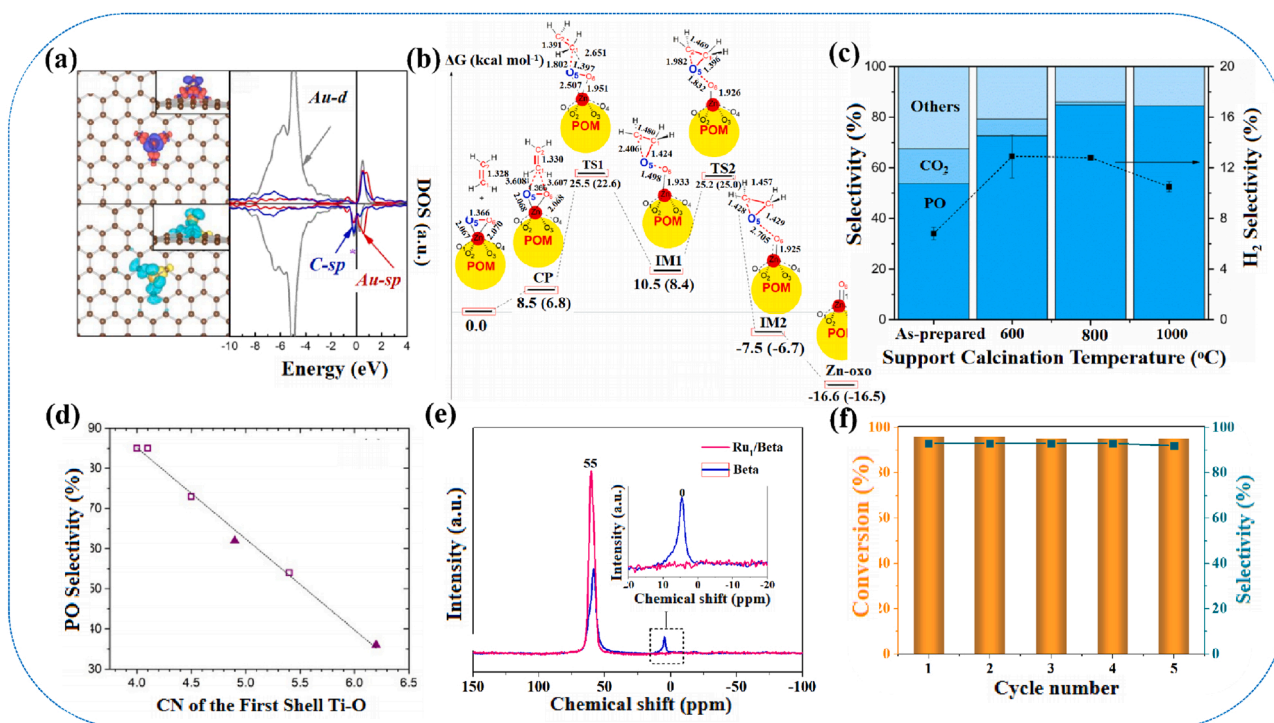


Fig. 9. (a) Structure and contour plots of differential charge density, spin density and DOS of AuSV [179]. (b) Calculated energy profile for the epoxidation of ethylene obtained by M06L/6-31 +G(d) calculations [180]. (c) Product selectivity and H₂ efficiency as a function of support calcination temperature. ("others" contains ethanal, acrolein, propanal, and acetone). Reaction conditions: reaction temperature 200 °C, $\text{H}_2/\text{C}_3\text{H}_6/\text{O}_2/\text{N}_2 = 3.5/3.5/3.5/24.5$ ml·min⁻¹, space velocity = 14,000 ml·h⁻¹·g⁻¹·cat⁻¹ [148]. (d) Selectivity as a function of Ti-O coordination number for propylene oxide [181]. (e) ²⁷Al MAS NMR spectra of Ru₁/Beta and Beta. (f) Recycling text of Ru₁/Beta for the catalytic epoxidation of styrene [185].

are between those of Ru(IV) and Ru(0), implying Ru atoms are positively charged. Extraframework AlOH was confirmed as the anchor sites for Ru atoms based on ^{27}Al magic angle spinning nuclear magnetic resonance (MAS NMR) measurements (Fig. 9e), the interaction between O atom in Al-OH groups and Ru guarantees the atomically dispersion of Ru, and the occupation of Al-OH also inhibits the occurrence of side reactions. The developed Ru₁/Beta catalyst showed superior styrene conversion, its TOF reaches 353 h^{-1} , which is much higher than that of Ru NPs/Beta and Beta. Moreover, the conversion of styrene and selectivity of styrene oxide are well retained after several recyclability (Fig. 9f). Then Tian et al. and Xiong et al. found Ag₁/mpg-C₃N₄ and Fe₁/CN were also efficient for the epoxidation of styrene [186,187]. DFT calculations indicated the adsorbed superoxide-like O₂ species favored its high activity, and the much lower reaction barrier to producing styrene oxide led to its high selectivity. The selective oxidation of alkenes over various catalysts are summarized in Table 3. Although so far not so many SACs have been reported for the epoxidation of alkenes, we believe SACs will provide more opportunities for alkenes epoxidation in the future. Specifically, the single metal center can interact with the double bond of alkene to form unique coordination structure, and thus obtaining epoxides with high selectivity.

4.4. CO oxidation

CO oxidation is an ideal probing reaction to discuss the fundamental steps for heterogeneous catalysis [189]. Because this reaction has one rate-determining step, and the only product of CO₂ has a much weaker interaction with the surface metals than does CO, thus it is convenient to measure and interpret the reaction data so as to understand the real catalytic process. In addition, owing to the effect of CO poisoning in the field of fuel cells, the preferential oxidation (PROX) of CO in H₂-rich streams is preferred, and various heterogeneous catalysts were investigated and developed for this reaction [190]. How to accelerate CO oxidation and prohibit the undesirable H₂ oxidation in a wide temperature region is crucial to control its selectivity. Both noble metals (Pt, Pd, Au, Ru, Rh etc.) and nonprecious transition metal (NTM) (Co₂O₃, CuO,

MnO₂, LaCoO₃ etc.) based catalysts have been employed for CO oxidation [191–193]. Wolf and co-workers also reviewed the understanding on the heterogeneous catalytic process of CO oxidation [194]. Several experimental factors including the ratio of O₂/CO, the partial pressure of CO, temperature, moisture can also influence the surface coverage of CO or O₂, and thus affecting their catalytic performance.

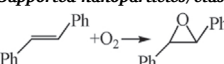
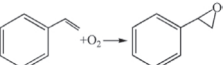
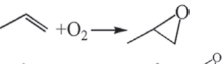
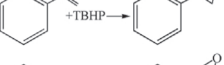
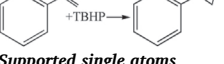
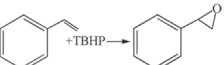
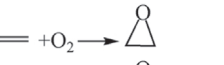
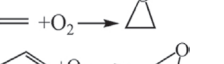
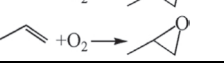

In 1990s, Haruta et al. discovered that the activity of CO oxidation catalyzed by supported Au catalyst increases with decreasing the particle size of Au below 4 nm [195–197], indicating CO oxidation is a structure-sensitive reaction. Considerable supported Au catalysts with different structures were developed in order to identify their active sites [108–110,198,199]. In 2008, Kiley and Hutchings et al. identified the active sites of Au/FeO_x catalysts for CO oxidation via utilizing HAADF-STEM, the activities of these investigated catalysts range from very low or no activity to very high. They found ~0.5 nm Au clusters play a dominant role for the superior activity for CO oxidation. Meanwhile, the Au clusters and nanoparticles that are too small (< 0.2 nm) or too large (> 5 nm) hardly contributed to the activity [200,201]. Moreover, The properties of support have an important effect on the catalytic behaviors of supported Au catalyst. Heiz et al. reported Au₈ clusters supported on MgO(100) with rich oxygen defects showed much higher activity than those supported on close-to-perfect.

magnesia surfaces, which can be ascribed to the charge transfer from MgO to the adsorbed Au cluster [202]. Besides, the thickness of MgO support could also affect the geometric structure of Au nanoclusters, resulting in different electronic interaction between MgO and Au, and thus exhibit different catalytic performance [203].

Anderson et al. reported CO oxidation catalyzed by Pd clusters/TiO₂ was size-selected [204]. The catalytic activity was correlated with the electronic structures, which was concluded through Pd 3d binding energy (BE) shifts relative to bulk Pd. From Fig. 10a, the activity of CO oxidation increased greatly from Pd₂ to Pd₄, then decreased when the size of cluster increased to Pd₇. For larger Pd clusters, the CO oxidation activity increased again with the cluster size increased to Pd₂₅. Meanwhile, there is a good correlation between the CO oxidation activity and Pd 3d BE shift, implying the electronic structures of Pd clusters play a

Table 3

The selective oxidation of various alkenes over different catalysts.

Reaction	Catalyst	T (°C)	P (bar)	Sel. (%)	Yield (μmol·g ⁻¹)	Ref.
Supported nanoparticles/clusters						
	Fe ₂ /mpg-C ₃ N ₄	90	-	91	-	[144] Nat. Commun. 2018
	Meso-Co ₃ O ₄	100	-	93	-	[145] Appl. Catal. B: Environ. 2018
	Ag ₃ /Al ₂ O ₃	110	1.33	50	-	[148] Science 2010
	AuNC@N-C	78	-	100	-	[174] ACS Catal. 2017
	Co-SnO ₂	80	-	75.5	17,200	[176] Catal. Sci. Technol. 2022
Supported single atoms						
	Ru ₁ /Beta	80	-	93	-	[185] ChemNanoMat 2020
	Au ₁ /Graphene	-	-	-	-	[179] Catal. Sci. Technol. 2016
	Zn ₁ /POM	-	-	-	-	[180] Inorg. Chem. 2017
	Au ₁ /TiO ₂	200	-	85	-	[181] J. Catal. 2019
	Co ₁ @Y	500	-	57	4700	[188] J. Am. Chem. Soc. 2022

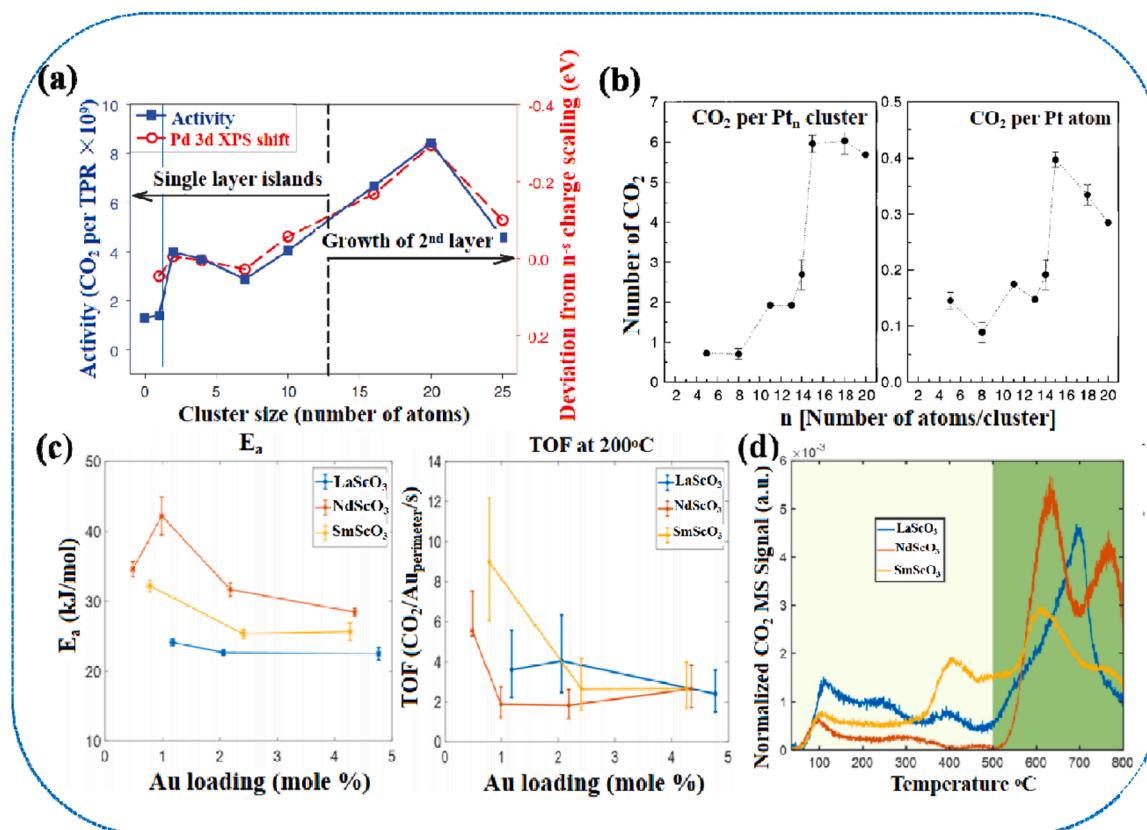


Fig. 10. (a) CO oxidation activity observed during temperature programmed reduction (TPR) (left axis, solid squares) compared with shifts in the Pd 3d binding energy, relative to expectations from smooth bulk scaling (right axis, open circles), as a function of cluster size [204]. (b) Left: Total number of catalytically produced CO₂ molecules as a function of cluster size. Right: Total number of produced CO₂ molecules per atom as a function of cluster size [205]. (c) Left: Activation energy of CO oxidation by Au on various supports. Arrhenius fits and the associated error bars were calculated from a linear least squares method. Right: The TOFs of CO oxidation catalyzed by Au on various supports at 200 °C, the errors were calculated using the standard deviations of the particle sizes [207]. (d) CO₂ TPD-MS results of the different supports normalized by the integrated CO₂ desorption [207].

significant role in their catalytic properties. Heiz et al. reported the produced CO₂ molecules over supported Pt clusters were also size-selected (Fig. 10b) [205]. When Pt_n clusters (n ≤ 8) were small, the production of CO₂ was very low. The CO oxidation activity increased substantially from Pt₁₁, the maximum amount of CO₂ was obtained on Pt₁₅. Local density functional (LDF) calculations revealed that these size-dependent catalytic performance is due to the difference of geometry and highest occupied molecular orbital (HOMO) energy. In addition, Pennington et al. investigated the effect of the size and intimacy of Au-Modified TiO₂ on photocatalytic CO oxidation, and found catalysts with large Au NPs and low Au||TiO₂ intimacy exhibit enhanced broadband activity [206].

Furthermore, the interactions between supports and active sites have a great influence on the catalytic properties of the catalysts being used for CO oxidation [207]. Marks et al. deposited Au on the oxide supports of LaScO₃, NdScO₃, and SmScO₃ with similar structure, and utilized CO oxidation as a probe reaction [208]. They found NdScO₃ exhibits a higher activation energy and a slower rate (Fig. 10c). Temperature-programmed desorption (TPD) measurements were carried out to verify the differences in their catalytic performance is associated with the CO₂ binding strength with the support surface (Fig. 10d), which can be ascribed to the discrepancies in the lanthanide cations' Lewis acidity, 4f electrons, and the inductive effect they impose. In addition, the preadsorbed surface CO molecules can facilitate the formation of reaction intermediates on the Au NPs/CeO₂ surface, and thus simplifying the reaction pathway and accelerating the reaction [209].

The mechanisms for CO oxidation on supported metal nanoparticles and SACs are different, owing to the different adsorption behaviors of

CO and O₂. Giving insights into the catalytic details of CO oxidation not only favors designing efficient catalysts to meet the requirements of industry, but also facilitates understanding the heterogeneous catalytic process. Trace amounts of water moisture in the reaction.

mixture can increase the catalytic activity in CO oxidation [210]. Lu et al. carried out experimental and theoretical studies to investigate the role of water in CO oxidation over Pt₁/CeO₂ [211]. And found water was not directly participate in the production of CO₂. They reported a water-mediated Mars-van Krevelen (MvK) mechanism for CO oxidation. The molecular water can be easily dissociated into hydroxyl, which reacts with CO to yield carboxyl intermediate, and subsequently decomposes to generate CO₂ and water with the aid of lattice hydroxyl (Fig. 11a). In addition, the presence of H₂ in the reaction feed can increase the CO oxidation activity compared with CO oxidation without H₂. One main reason is that H₂ can contribute to the formation of oxygen vacancies on the reducible supports [212]. Heiz et al. proposed a reaction mechanism of CO oxidation over Pd clusters, and found negligible CO₂ was produced in low-temperature region (Fig. 11b) [213]. When the reaction temperature was increased to 300 K, the O₂ molecule can be activated on the exposed Pd atoms in Pd clusters, and reacted with the adsorbed CO, obeying a Langmuir-Hinshelwood (L-H) mechanism. It is noteworthy that larger Pd clusters were active for CO oxidation at T > 400 K, which might because more Pd atoms in larger Pd clusters are exposed to O₂, and thus facilitating CO oxidation. Behm et al. carried out kinetic model to confirm the selective oxidation of CO on γ-Al₂O₃ supported Pt particles followed L-H mechanism [214]. Belver et al. reported the reaction mechanism of CO PROX over oxidized copper-ceria catalysts was redox MvK via operando spectroscopic studies [215]. Thus a

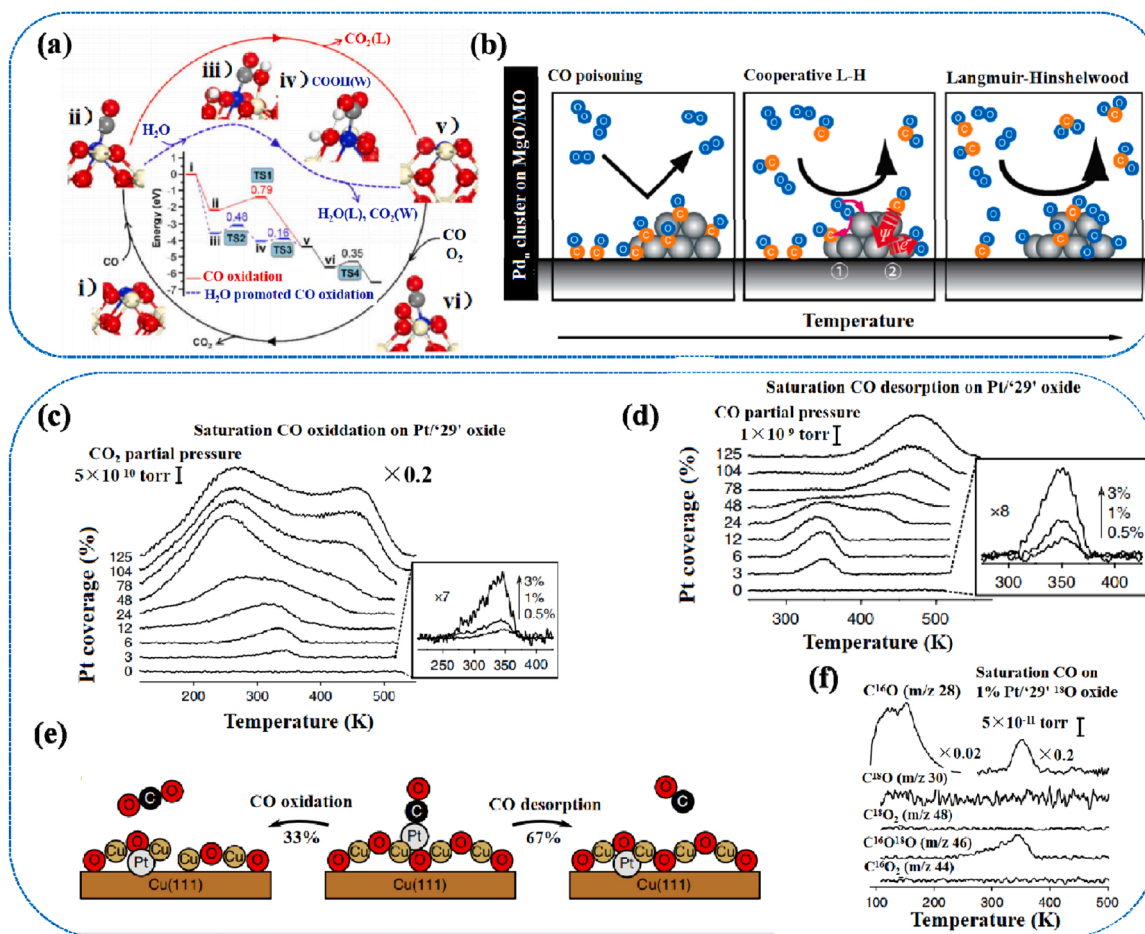


Fig. 11. (a) The proposed reaction pathways for CO oxidation and H₂O promoted CO oxidation on Pt₁/CeO₂(110). Here the structures of intermediates and transition states (TS) of the key elementary steps are present. The inset in the reaction cycles shows the calculated energy profile in eV. After one catalytic cycle in both cases, the catalyst is recovered and releases two CO₂ molecules. The yellow, blue, red, gray, and white spheres represent Ce, Pt, O, C, and H atoms, respectively [211]. (b) Mechanism of CO oxidation on Pd clusters from low to high temperature. At low temperature, Pd clusters will be poisoned by CO and cannot catalyze the CO oxidation. When the temperature increases to ca. 300 K, part of the Pd clusters are exposed to O₂ molecules and become able to activate O₂ and catalyze the CO+O₂ reaction. At ca. 400 K, a L-H-type reaction can be observed on Pd clusters for CO oxidation [213]. (c) A family of TPD curves of CO₂ (m/z 44) desorption from saturation CO coverages at different Pt coverages on the '29' oxide. (d) A family of TPD curves of CO (m/z 28) desorption from the same experiments as in (a). The insets highlight low Pt coverages at which Pt exists as isolated atoms. (e) Schematic of the competing pathways for CO oxidation and CO desorption. (f) TPD after saturation C¹⁶O exposure on a monolayer with 1% Pt coverage supported on an ¹⁸O-labeled '29' oxide [219].

model catalyst with definite structure should be established to further study the intrinsic mechanism of this model catalytic reaction.

Since Haruta et al. discovered the ultra high activity of Au catalysts for low-temperature CO oxidation, considerable Au catalysts with different structures were developed in order to identify their active sites. Utilizing appropriate oxide supports, Au SACs can be as active as Au NPs [216]. In addition, Au SACs show much higher specific activity and stability in CO oxidation due to their maximized atomic utilization and strong metal-support interaction (MSI), respectively [217]. Liu et al. demonstrated Au₁/FeO_x are much more sintering resistant than Au NPs/FeO_x for CO oxidation, and exhibited extremely high reaction stability in a wide temperature range [218]. This superior stability resulted from the strong covalent MSI between Au atoms and FeO_x support. And Au₁/CeO₂ catalyst was highly active and selective for CO-PROX, because Au₁/CeO₂ was unable to dissociate the adsorbed H₂, and thus was inert to activate H₂.

Sykes et al. designed a model system of Pt₁/Cu₂O for CO oxidation at low temperatures, and utilized TPD to investigate the activity and mechanism [219]. It can be observed from Fig. 11c that the amount of produced CO₂ increases with the increase of Pt coverage, with a peak maximum at 345 K. The CO desorption peak is located at 350 K (Fig. 11d). CO desorption and oxidation coexist under realistic reaction

conditions, both of which can result in the diffusion of Pt below the oxide surface (Fig. 11e). Isotope labeling experiments were carried out to probe CO oxidation mechanism. The monitored results indicated the formed CO₂ was exclusively m/z 46, directly evidencing a MvK oxidation mechanism. That is, the lattice oxygen from Cu₂¹⁸O-like support reacts with C¹⁶O to form C¹⁶O¹⁸O (Fig. 11f). Qiao et al. reported that Pt₁/FeO_x catalyst was highly efficient for CO oxidation and CO-PROX reactions [220]. DFT calculations indicate O₂ is activated at the O vacancy site of Pt₁/FeO_x, and the positively charged Pt atoms can adsorb and activate CO much easier than Pt clusters. Nevertheless, when Pt single atoms were dispersed on the inert supports such as Al₂O₃ [221], the TOF of Pt NPs was about four-fold higher than that of Pt₁/Al₂O₃, suggesting not all the SACs are much more efficient than the corresponding NPs in the heterogeneous catalysis, comprehensive factors need to be considered so as to obtain an optimal catalyst for the desired reaction [222]. The CO oxidation and CO-PROX over various catalysts are summarized in Table 4.

5. Comparison of the catalytic behavior of nanoparticles and single atoms

As discussed before, different types of supported metal catalysts

Table 4

The CO oxidation and CO-PROX over various catalysts.

Reaction	Catalyst	T (°C)	P (bar)	Sel. (%)	Yield ($\mu\text{mol}\cdot\text{g}^{-1}$)	Ref.
Supported nanoparticles/clusters						
CO PROX	Au NPs/ Al_2O_3	-70	-	-	-	[193] <i>J. Catal.</i> 1989
CO PROX	Au NPs/ TiO_2	0	-	-	-	[194] <i>J. Catal.</i> 1993
$\text{CO} + \text{O}_2 \rightarrow \text{CO}_2$	Au NPs/ $\text{MO}_x\text{-Al}_2\text{O}_3$	-40	-	100	-	[109] <i>Chinese J. Catal.</i> 2002
$\text{CO} + \text{O}_2 \rightarrow \text{CO}_2$	Au NPs/ NiFe_2O_4	-22	-	100	-	[196] <i>Chin. Sci. B</i> 2001
$\text{CO} + \text{O}_2 \rightarrow \text{CO}_2$	Au NPs/ ZnO	-	-	100	-	[110] <i>Appl. Catal. A</i> 2001
$\text{CO} + \text{O}_2 \rightarrow \text{CO}_2$	Au NPs/ Fe_2O_3	-22	-	100	-	[197] <i>Appl. Catal. A</i> 2001
CO PROX	CoO_x NPs/ CeO_2	100	-	100	-	[187] <i>Appl. Catal. B: Environ.</i> 2012
CO PROX	Pt NPs/ Al_2O_3	150	0.8	15	-	[214] <i>J. Catal.</i> 1997
CO PROX	CuO-CeO_2	177	-	100	-	[215] <i>Top. Catal.</i> 2009
Supported single atoms						
$\text{CO} + \text{O}_2 \rightarrow \text{CO}_2$	Au_1/FeO_x	200	-	100	-	[216] <i>Chinese J. Catal.</i> 2016
$\text{CO} + \text{O}_2 \rightarrow \text{CO}_2$	Au_1/FeO_x	24	-	100	9000	[217] <i>Nano Res.</i> 2015
CO PROX	Au_1/CeO_2	50	-	100	45,900	[218] <i>ACS Catal.</i> 2015
CO PROX	Pt_1/FeO_x	27	-	100	67,600	[220] <i>ACS Catal.</i> 2015
$\text{CO} + \text{O}_2 \rightarrow \text{CO}_2$	$\text{Pt}_1/\theta\text{-Al}_2\text{O}_3$	176	-	100	-	[221] <i>J. Am. Chem. Soc.</i> 2013
$\text{CO} + \text{O}_2 \rightarrow \text{CO}_2$	Pt_1/CeO_2	200	1	100	-	[223] <i>Angew. Chem.</i> 2022
$\text{CO} + \text{O}_2 \rightarrow \text{CO}_2$	Au_1/NiO	120	1	100	-	[224] <i>ACS Catal.</i> 2022
$\text{CO} + \text{O}_2 \rightarrow \text{CO}_2$	$\text{Cu}_1/\text{CeO}_2\text{-TiO}_2$	250	1	100	-	[225] <i>ACS Catal.</i> 2021
$\text{CO} + \text{O}_2 \rightarrow \text{CO}_2$	Pd_1/CeO_2	100	1	100	0	[226] <i>ACS Catal.</i> 2020

involving nanoparticles, clusters and single atoms have been shown to be active and selective for the heterogeneous selective oxidation reactions such as selective oxidation of methane, aerobic selective oxidation of alcohols, epoxidation of alkenes and CO oxidation. Their catalytic behaviors are directly associated with the electronic structure of metal species as well as the surface arrangement of support. When revisiting these reports, some inconsistent conclusions were reached on the active sites and intrinsic activity of metal nanoparticles, clusters and single atoms. Such as the function of under-coordinated metal sites is different in oxidation of alcohol and epoxidation of alkene. What we emphasized was that the catalytic activity should be compared under the same or at least similar reaction conditions. Otherwise, it is meaningless to discuss the different catalytic performance of nanoparticles, clusters and single atoms. In addition, there are dynamic structural transformations between nanoparticles, clusters and single atoms, whose state depends on the reaction conditions. Thus, the establishment of the reactivity-structure relationships should consider the real catalytic species during reaction process. The different catalytic behavior of nanoparticles, clusters and atomically dispersed metal species can also be explained from a mechanistic point of view. One is related to the interface of metal-substrate, which has been discussed intensively, and is regarded as the origin of different activity [227-230]. Another is the interaction between each component, which modify their electronic structure caused by charge transfer [231,232].

6. Conclusions and prospects

In summary, the selective oxidation reactions are of great significance for both fine chemical and petrochemical industries, yet when two or multiple reaction paths coexist, the selectivity of the target product remains challenging. Recent advances in four challenging catalytic oxidation reactions are discussed and summarized in this review: selective oxidation of methane to methanol, aerobic oxidation of alcohols to aldehydes or ketones, epoxidation of alkenes to epoxide, and preferential oxidation of carbon monoxide in hydrogen to CO_2 . The common characteristics of these four types of reactions are that their high selectivity derives from the moderate adsorption of reactants and the rapid desorption of the target product. Tremendous efforts have been devoted to developing efficient catalytic materials which range from nanoparticles, nanoclusters to single atoms for these transformations. And we summarized the important factors that affected the performance of each catalytic system from a catalytic point of view, including the adsorption of substrates on supported metal nanoparticles and single

atoms, the activation of O_2 , the characteristics of catalyst (size and shape of metal particles, metal-support interaction, and the nature of the support). These will provide some thoughts and guidance for the design of efficient catalytic system following the optimal reaction path to obtain target product in the heterogeneous selective oxidation reactions.

Although numerous advances have been made in the heterogeneous selective oxidation reactions using nanoparticles, nanoclusters and single atom catalysts, some challenges are yet to be addressed: (a) Achieving both high activity and selectivity. For the heterogeneous selective oxidation reactions, the high selectivity is often achieved at the cost of activity. When the size of metal particles is reduced from nanoparticles, nanoclusters to single atoms, these geometric structure variation leads to the alteration of electronic structure and binding capacities. That is, the adsorption of both the product molecules and reactant molecules will be weakened. Therefore, novel catalytic systems (such as the bifunctional catalysts: single atom alloy) need to be developed to break this “seesaw effect”. (b) Gaining insights into the dynamic characteristics during the catalytic process, which will cover the evolution of metal properties (geometric and electronic structures), support properties (electronic structure and surface arrangement), and the interaction between metal and reactant/solvent. The closer to the real catalytic reaction process, the better to understand the real structure-activity relationship and catalytic reaction mechanism. This relies on advanced in-situ/operando spectroscopic characterization technologies, reaction kinetics, as well as theoretical studies (machine learning and artificial intelligence), the developed single atom catalysts with well-defined structure and uniform active center provide ideal platforms to carry out these investigations, but it is still challenging to track the catalyst evolution during reaction process under severe and complex reaction conditions. Actually, the heterogeneous selective oxidation reaction is not only dependent on the active site structure but also on oxygen coverage, deep oxidation can also occur at a relatively high oxygen coverage. Therefore, making clear how the oxygen coverage and reaction rate are influenced by the active site structure or reaction parameters is also important.

Overall, to gain a unified knowledge on heterogeneous selective oxidation, we outlined from a catalytic point of view of the adsorption, activation and four types of selective oxidation reactions over supported metal nanoparticles, clusters and single atoms. All of them are based on electronic interactions, multidisciplinary knowledge including physical chemistry of surface, solid-state chemistry, and chemical reactivity can be intersected to achieve a comprehensive explanation.

Declaration of Competing Interest

The authors declare that they have no known competing financial interests or personal relationships that could have appeared to influence the work reported in this paper.

Data availability

Data will be made available on request.

Acknowledgments

This work was financially supported by the R&D Program of Beijing Municipal Education Commission (KJZD20191443001), the National Natural Science Foundation of China (22202014, 22176189, 22206185), the National Environmental Protection Standard Project (JZ2022-012), the Fund Project of Beijing Municipal Research Institute of Eco-Environmental Protection (Y2023-005), Beijing Municipal Science and Technology Commission (Z181100000118003), the Youth Innovation Promotion Association of Chinese Academy of Sciences and the Fundamental Research Funds for the Central Universities.

References

- [1] C.N. Dai, J. Zhang, C.P. Huang, Z.G. Lei, Ionic liquids in selective oxidation: catalysts and solvents, *Chem. Rev.* 117 (2017) 6929–6983.
- [2] Z. Guo, B. Liu, Q.H. Zhang, W.P. Deng, Y. Wang, Y.H. Yang, Recent advances in heterogeneous selective oxidation catalysis for sustainable chemistry, *Chem. Soc. Rev.* 43 (2014) 3480–3524.
- [3] R.K. Grasselli, Fundamental principles of selective heterogeneous oxidation catalysis, *Top. Catal.* 21 (2002) 79–88.
- [4] Y. Xiong, W.M. Sun, Y.H. Han, P.Y. Xin, X.S. Zheng, W.S. Yan, J.C. Dong, J. Zhang, D.S. Wang, Y.D. Li, Cobalt single atom site catalysts with ultrahigh metal loading for enhanced aerobic oxidation of ethylbenzene, *Nano Res.* 14 (2021) 2418–2423.
- [5] Z.Q. Hou, L.Y. Dai, J.G. Deng, G.F. Zhao, L. Jing, Y.S. Wang, X.H. Yu, R.Y. Gao, X. R. Tian, H.X. Dai, D.S. Wang, Y.X. Liu, Electronically engineering water resistance in methane combustion with an atomically dispersed tungsten on PdO catalyst, *Angew. Chem. Int. Ed.* 61 (2022) 202201655–202201663.
- [6] X.B. Zheng, B.B. Li, Q.H. Wang, D.S. Wang, Y.D. Li, Emerging low-nuclearity supported metal catalysts with atomic level precision for efficient heterogeneous catalysis, *Nano Res.* 15 (2022) 7806–7839.
- [7] A.J.C. Wahart, J. Staniland, G.J. Miller, S.C. Cosgrove, Oxidase enzymes as sustainable oxidation catalysts, *R. Soc. Open Sci.* 9 (2021) 211572–211588.
- [8] C.M. Friend, B.J. Xu, Heterogeneous catalysis: a central science for a sustainable future, *Acc. Chem. Res.* 50 (2017) 517–521.
- [9] X. Liu, Y. Maegawa, Y. Goto, K. Hara, S. Inagaki, Heterogeneous catalysis for water oxidation by an iridium complex immobilized on bipyridine-periodic mesoporous organosilica, *Angew. Chem. Int. Ed.* 55 (2016) 7943–7947.
- [10] J.Y. Xu, G.J. Shi, Y.X. Liang, Q.T. Lu, L.J. Ji, Selective aerobic oxidation of toluene to benzaldehyde catalyzed by covalently anchored N-hydroxyphthalimide and cobaltous ions, *Mol. Catal.* 503 (2021) 111440–111449.
- [11] T. Shamim, D. Choudhary, S. Mahajan, G. Rajive, P. Satya, Covalently anchored metal complexes onto silica as selective catalysts for the liquid phase oxidation of benzoin to benzils with air, *Catal. Commun.* 20 (2009) 1931–1935.
- [12] R. Serra-Maia, F.M. Michel, Y.J. Kang, E.A. Stach, Decomposition of hydrogen peroxide catalyzed by AuPd nanocatalysts during methane oxidation to methanol, *ACS Catal.* 10 (2020) 5115–5123.
- [13] J. Teržana, P. Djinović, J. Zavašnik, I. Arčon, G. Žerjav, M. Spreitzer, A. Pintar, Alkali and earth alkali modified CuO_x/SiO₂ catalysts for propylene partial oxidation: what determines the selectivity? *Appl. Catal. B Environ.* 237 (2018) 214–227.
- [14] C.H. Wu, C. Liu, D. Su, H.L. Xin, H.T. Fang, B. Eren, S. Zhang, C.B. Murray, M. B. Salmeron, Bimetallic synergy in cobalt–palladium nanocatalysts for CO oxidation, *Nat. Catal.* 2 (2019) 78–85.
- [15] Z.K. Zhao, H.L. Yang, Y. Li, X.W. Guo, Cobalt-modified molybdenum carbide as an efficient catalyst for chemoselective reduction of aromatic nitro compounds, *Green Chem.* 16 (2014) 1274–1281.
- [16] R. Serra-Maia, F.M. Michel, T.A. Douglas, Y.J. Kang, E.A. Stach, Mechanism and kinetics of methane oxidation to methanol catalyzed by AuPd nanocatalysts at low temperature, *ACS Catal.* 11 (2021) 2837–2845.
- [17] G. Hamm, T. Schmidt, J. Breitbach, D. Franke, C. Becker, K. Wandelt, The adsorption of ethene on Pd(111) and ordered Sn/Pd(111) surface alloys, *Surf. Sci.* 223 (2009) 209–232.
- [18] T. Lear, R. Marshall, J. Antonio, L. Sanchez, S.D. Jackson, The application of infrared spectroscopy to probe the surface morphology of alumina-supported palladium catalysts, *J. Chem. Phys.* 123 (2005) 174706–174718.
- [19] B.T. Qiao, A.Q. Wang, X.F. Yang, L.F. Allard, Z. Jiang, Y.T. Cui, J.Y. Liu, J. Li, T. Zhang, Single-atom catalysis of CO oxidation using Pt₁/FeO_x, *Nat. Chem.* 3 (2011) 634–641.
- [20] X.F. Yang, A.Q. Wang, B.T. Qiao, J. Li, J.Y. Liu, T. Zhang, Single-atom catalysts: a new frontier in heterogeneous catalysis, *Acc. Chem. Res.* 46 (2013) 1740–1748.
- [21] Z. Li, S.F. Ji, Y.W. Liu, X. Cao, S.B. Tian, Y.J. Chen, Z.Q. Niu, Y.D. Li, Well-defined materials for heterogeneous catalysis: from nanoparticles to isolated single-atom sites, *Chem. Rev.* 120 (2020) 623–682.
- [22] J.M. Basset, A. Choplin, Surface organometallic chemistry: a new approach to heterogeneous catalysis? *J. Mol. Catal.* 21 (1983) 95–108.
- [23] C. Coppyret, M. Chabanas, R. Petroff, S. Arroman, J.M. Basset, Homogeneous and heterogeneous catalysis: bridging the gap through surface organometallic chemistry, *Angew. Chem. Int. Ed.* 42 (2003) 156–181.
- [24] C.P. Nicholas, H. Ahn, T.J. Marks, Synthesis, spectroscopy, and catalytic properties of cationic organozirconium adsorbates on “super acidic” sulfated alumina. “single-site” heterogeneous catalysts with virtually 100% active sites, *J. Am. Chem. Soc.* 125 (2003) 4325–4331.
- [25] J.M. Thomas, R. Raja, D.W. Lewis, Single-site heterogeneous catalysts, *Angew. Chem. Int. Ed.* 44 (2005) 6456–6482.
- [26] A.Q. Wang, J. Li, T. Zhang, Heterogeneous single-atom catalysis, *Nat. Rev. Chem.* 2 (2018) 65–81.
- [27] E. Grifoni, G. Piccini, J.A. Lercher, V.A. Glezakou, R. Rousseau, M. Parrinello, Confinement effects and acid strength in zeolites, *Nat. Commun.* 12 (2021) 2630–2638.
- [28] Y.C. Chai, W.L. Dai, G.J. Wu, N.J. Guan, L.D. Li, Confinement in a zeolite and zeolite catalysis, *Acc. Chem. Res.* 54 (2021) 2894–2904.
- [29] R.X. Zhang, X. Shi, Y.F. Wang, Y.X. Jin, Z.F. Yan, Z.H. Gao, W. Huang, L. Liu, Z. J. Zuo, Importance of edge and corner sites on CeO₂ nanoparticles for direct conversion of methane to methanol, *ACS Appl. Nano Mater.* 5 (2022) 12600–12606.
- [30] N. Pantha, K. Ulman, S. Narasimhan, Adsorption of methane on single metal atoms supported on graphene: role of electron back-donation in binding and activation, *J. Chem. Phys.* 153 (2020) 244701–244713.
- [31] V. Fung, G.X. Hu, F. Tao, D.E. Jiang, Methane chemisorption on oxide-supported Pt single atom, *ChemPhysChem* 20 (2019) 2217–2220.
- [32] M. Asai, A. Takahashi, Y. Jiang, M. Ishizaki, M. Kurihara, T. Kawamoto, Trace alcohol adsorption by metal hexacyanocobaltate nanoparticles and the adsorption mechanism, *J. Phys. Chem. C* 122 (2018) 11918–11925.
- [33] M.T. Nayakasinghe, N. Sivapragasam, U. Burghaus, Adsorption of alcohols on a two-dimensional SiO₂ single crystal-alcohol adsorption on silicatenes, *Chem. Phys. Lett.* 689 (2017) 105–110.
- [34] A.M. Doyle, S.K. Shaikhutdinov, H.J. Freund, Alkene chemistry on the palladium surface: nanoparticles vs single crystals, *J. Catal.* 223 (2004) 444–453.
- [35] J. Hulva, M. Meier, R. Blum, Z. Jakub, F. Kraushofer, M. Schmid, U. Diebold, C. Franchini, G.S. Parkinson, Unraveling CO adsorption on model single-atom catalysts, *Science* 371 (2021) 375–379.
- [36] C.D. Zeinalipour-Yazdi, D.J. Willock, L. Thomas, K. Wilson, A.F. Lee, CO adsorption over Pd nanoparticles: a general framework for IR simulations on nanoparticles, *Surf. Sci.* 646 (2016) 210–220.
- [37] Y.G. Ptushinskii, Low-temperature adsorption of gases on metal surfaces (Review), *J. Low. Temp. Phys.* 30 (2004) 1–26.
- [38] L.L. Cao, Q.Q. Luo, J.J. Chen, L. Wang, Y. Lin, H.J. Wang, X.K. Liu, X.Y. Shen, W. Zhang, W. Liu, Z.M. Qi, Z. Jiang, J.L. Yang, T. Yao, Dynamic oxygen adsorption on single-atomic ruthenium catalyst with high performance for acidic oxygen evolution reaction, *Nat. Commun.* 10 (2019) 4849–4857.
- [39] D.Y. Kuo, J.K. Kawasaki, J.N. Nelson, J. Kloppenburg, G. Hautier, K.M. Shen, D. G. Schlom, J. Suntivich, Influence of surface adsorption on the oxygen evolution reaction on IrO₂(110), *J. Am. Chem. Soc.* 139 (2017) 3473–3479.
- [40] P. Chaudhuri, C.N. Verani, E. Bill, E. Bothe, T. Weyhermüller, K. Wieghardt, Electronic structure of bis(σ-iminobenzosequinoxonato)metal complexes (Cu, Ni, Pd). The art of establishing physical oxidation states in transition-metal complexes containing radical ligands, *J. Am. Chem. Soc.* 123 (2001) 2213–2223.
- [41] K.B. Zhou, Y.D. Li, Catalysis based on nanocrystals with well-defined facets, *Angew. Chem. Int. Ed.* 51 (2012) 602–613.
- [42] P. Strasser, S. Koh, T. Anniyev, J. Greeley, K. More, C.F. Yu, Z.C. Liu, S. Kaya, D. Nordlund, H. Ogasawara, M.F. Toney, A. Nilsson, Lattice-strain control of the activity in dealloyed core–shell fuel cell catalysts, *Nat. Chem.* 2 (2010) 454–460.
- [43] K.L. Kelly, E. Coronado, L.L. Zhao, G.C. Schatz, The optical properties of metal nanoparticles: the influence of size, shape, and dielectric environment, *J. Phys. Chem. B* 107 (2003) 668–677.
- [44] K.B. Zhou, R.P. Wang, B.Q. Xu, Y.D. Li, Synthesis, characterization and catalytic properties of CuO nanocrystals with various shapes, *Nanotech* 17 (2006) 3939–3943.
- [45] N. Dimitratos, A. Villa, D. Wang, F. Porta, D.S. Su, L. Prati, Pd and Pt catalysts modified by alloying with Au in the selective oxidation of alcohols, *J. Catal.* 244 (2006) 113–121.
- [46] D.A. Slanac, W.G. Hardin, K.P. Johnston, K.J. Stevenson, Atomic ensemble and electronic effects in Ag-Rich AgPd nanoalloy catalysts for oxygen reduction in alkaline media, *J. Am. Chem. Soc.* 134 (2012) 9812–9819.
- [47] M.M. Montemore, M.A. Spronsen, R.J. Madix, C.M. Friend, O₂ activation by metal surfaces: implications for bonding and reactivity on heterogeneous catalysts, *Chem. Rev.* 118 (2018) 2816–2862.
- [48] U.J. Etim, P. Bai, O.M. Gazit, Z.Y. Zhong, Low-Temperature Heterogeneous Oxidation Catalysis and Molecular Oxygen Activation, *Catal. Rev. Sci. Eng.* (2021), <https://doi.org/10.1080/01614940.2021.1919044>.

- [49] A. Bielanski, J. Haber, *Oxygen in Catalysis*, CRC Press, Boca Raton/New York, 1990, <https://doi.org/10.1201/9781482293289>.
- [50] Q.H. Shang, N.F. Tang, H.F. Qi, S. Chen, G.L. Xu, C.Y. Wu, X.L. Pan, X.D. Wang, Y. Cong, A palladium single-atom catalyst toward efficient activation of molecular oxygen for cinnamyl alcohol oxidation, *Chin. J. Catal.* 41 (2020) 1812–1817.
- [51] X.Y. Deng, B.K. Min, A. Guloy, C.M. Friend, Enhancement of O₂ dissociation on Au(111) by adsorbed oxygen: implications for oxidation catalysis, *J. Am. Chem. Soc.* 127 (2005) 9267–9270.
- [52] P. Concepción, M. Boronat, S. García-García, E. Fernández, A. Corma, Enhanced stability of Cu clusters of low atomicity against oxidation. Effect on the catalytic redox process, *ACS Catal.* 7 (2017) 3560–3568.
- [53] F. Wang, Z. Li, H.H. Wang, M. Chen, C.B. Zhang, P. Ning, H. He, Nano-sized Ag rather than single-atom Ag determines CO oxidation activity and stability, *Nano Res.* 15 (2022) 452–456.
- [54] X.L. Wang, H. Xiao, A. Li, Z. Li, S.J. Liu, Q.H. Zhang, Y. Gong, L.R. Zheng, Y. Q. Zhu, C. Chen, D.S. Wang, Q. Peng, L. Gu, X.D. Han, J. Li, Y.D. Li, Constructing NiCo/Fe₃O₄ heteroparticles within MOF-74 for efficient oxygen evolution reactions, *J. Am. Chem. Soc.* 140 (2018) 15336–15341.
- [55] M. Boronat, A. Corma, Oxygen activation on gold nanoparticles: separating the influence of particle size, particle shape and support interaction, *Dalton Trans.* 39 (2010) 8538–8546.
- [56] P. Concepción, M. Boronat, S. García-García, E. Fernández, A. Corma, Enhanced stability of Cu clusters of low atomicity against oxidation. Effect on the catalytic redox process, *ACS Catal.* 7 (2017) 3560–3568.
- [57] E. Fernández, M. Boronat, A. Corma, Trends in the reactivity of molecular O₂ with copper clusters. influence of size and shape, *J. Phys. Chem. C* 119 (2015) 19832–19846.
- [58] Y.F. Li, U. Aschauer, J. Chen, A. Selloni, Adsorption and reactions of O₂ on anatase TiO₂, *Acc. Chem. Res.* 47 (2014) 3361–3368.
- [59] W.J. Yang, Y.F. Zhu, F. You, L. Yan, Y.J. Ma, C.Y. Lu, P.Q. Gao, Q. Hao, W.L. Li, Insights into the surface-defect dependence of molecular oxygen activation over birnessite-type MnO₂, *Appl. Catal. B: Environ.* 233 (2018) 184–193.
- [60] X.F. Ma, H.L. Xin, Orbitalwise coordination number for predicting adsorption properties of metal nanocatalysts, *PRL* 118 (2017) 036101–036105.
- [61] F. Calle-Vallejo, D. Loffreda, M.T.M. Koper, P. Sautet, Introducing structural sensitivity into adsorption-energy scaling relations by means of coordination numbers, *Nat. Chem.* 7 (2015) 403–410.
- [62] J.W. Huang, S. He, J.L. Goodsell, J.R. Mulcahy, W.X. Guo, A. Angerhofer, W. D. Wei, Manipulating atomic structures at the Au/TiO₂ interface for O₂ activation, *J. Am. Chem. Soc.* 142 (2020) 6456–6460.
- [63] Y.L. Zhang, J.Y. Zhang, B.S. Zhang, R. Si, B. Han, F. Hong, Y.M. Niu, L. Sun, L. Li, B.T. Qiao, K.J. Sun, J.H. Huang, M. Haruta, Boosting the catalysis of gold by O₂ activation at Au-SiO₂ interface, *Nat. Commun.* 11 (2020) 558–567.
- [64] C.Y. Jia, W.H. Zhong, M.S. Deng, J. Jiang, Microscopic insight into the activation of O₂ by Au nanoparticles on ZnO(101) support, *J. Phys. Chem. C* 120 (2016) 4322–4328.
- [65] S. Han, J.E. E. Jr, G.M. Mullen, C.B. Mullins, H₂O-improved O₂ activation on the Pd–Au bimetallic surface, *Chem. Commun.* 53 (2017) 3990–3993.
- [66] J.T. Roberts, R.J. Madix, Epoxidation of olefins on silver: conversion of norbornene to norbornene oxide by atomic oxygen on Ag(110), *J. Am. Chem. Soc.* 110 (1988) 8540–8541.
- [67] S. Linic, M.A. Barteau, Formation of a stable surface oxametallacycle that produces ethylene oxide, *J. Am. Chem. Soc.* 124 (2002) 310–317.
- [68] M.O. Özbek, R.A. Santen, The mechanism of ethylene epoxidation catalysis, *Catal. Lett.* 143 (2013) 131–141.
- [69] Q. Zhang, Y.L. Guo, W.C. Zhan, Y. Guo, L. Wang, Y.S. Wang, G.Z. Lu, Gas-phase epoxidation of propylene by molecular oxygen over Ag–Cu–Cl/BaCO₃ catalyst: effects of Cu and Cl loadings, *Chin. J. Catal.* 38 (2017) 65–72.
- [70] J. Terzan, M. Hus, B. Likozar, P. Djinić, Propylene epoxidation using molecular oxygen over copper- and silver-based catalysts: a review, *ACS Catal.* 10 (2020) 13415–13436.
- [71] T.B. Li, F. Liu, Y. Tang, L. Li, S. Miao, Y. Su, J.Y. Zhang, J.H. Huang, H. Sun, M. Haruta, A.Q. Wang, B.T. Qiao, J. Li, T. Zhang, Maximizing the number of interfacial sites in single-atom catalysts for the highly selective, solvent-free oxidation of primary alcohols, *Angew. Chem. Int. Ed.* 57 (2018) 7795–7799.
- [72] R. Coquet, K.L. Howard, D.J. Willock, Theory and simulation in heterogeneous gold catalysis, *Chem. Soc. Rev.* 37 (2008) 2046–2076.
- [73] G. Sitja, S.L. Moal, M. Marsault, G. Hamm, F.R. Leroy, C.R. Henry, Transition from molecule to solid state: reactivity of supported metal clusters, *Nano Lett.* 13 (2013) 1977–1982.
- [74] Y. Lei, H. Zhao, R.D. Rivas, S. Lee, B. Liu, J. Lu, E. Stach, R.E. Winans, K. W. Chapman, J.P. Greeley, Adsorbate-induced structural changes in 1–3 nm platinum nanoparticles, *J. Am. Chem. Soc.* 136 (2014) 9320–9326.
- [75] M.A. Newton, C. Belver-Coldeira, A. Martínez-Arias, M. Fernández-García, Dynamic in situ observation of rapid size and shape change of supported Pd nanoparticles during CO/N₂ cycling, *Nat. Mater.* 6 (2007) 528–532.
- [76] Y. Nagai, K. Dohmae, Y. Ikeda, N. Takagi, T. Tanabe, N. Hara, G. Guilera, S. Pascarelli, M.A. Newton, O. Kuno, In situ redispersion of platinum autoexhaust catalysts: an on-line approach to increasing catalyst lifetimes? *Angew. Chem. Int. Ed.* 47 (2008) 9303–9306.
- [77] M. Moliner, J.E. Gabay, C.E. Kliewer, R.T. Carr, J. Guzman, G.L. Casty, P. Serna, A. Corma, Reversible transformation of Pt nanoparticles into single atoms inside high-silica chabazite zeolite, *J. Am. Chem. Soc.* 138 (2016) 15743–15750.
- [78] L.C. Liu, A. Corma, Metal catalysts for heterogeneous catalysis: from single atoms to nanoclusters and nanoparticles, *Chem. Rev.* 118 (2018) 4981–5079.
- [79] B.A. Arndtsen, R.G. Bergman, T.A. Mobley, T.H. Peters, Selective intermolecular carbon-hydrogen bond activation by synthetic metal complexes in homogeneous solution, *Acc. Chem. Res.* 28 (1995) 154–162.
- [80] P. Tomkins, M. Ranocchiari, J.A. Bokhoven, Direct conversion of methane to methanol under mild conditions over Cu-zeolites and beyond, *Acc. Chem. Res.* 50 (2017) 418–425.
- [81] S. Grundner, M.A.C. Markovits, G. Li, M. Tromp, E.A. Pidko, E.J.M. Hensen, A. Jentys, M. Sanchez-Sanchez, J.A. Lercher, Single-site trinuclear copper oxygen clusters in mordenite for selective conversion of methane to methanol, *Nat. Commun.* 6 (2015) 7546–7554.
- [82] K. Narsimhan, K. Iyoki, K. Dinh, Y. Roman-Leshkov, Catalytic oxidation of methane into methanol over copper-exchanged zeolites with oxygen at low temperature, *ACS Cent. Sci.* 2 (2016) 424–429.
- [83] V.L. Sushkevich, D. Palagin, M. Ranocchiari, J.A. Bokhoven, Selective anaerobic oxidation of methane enables direct synthesis of methanol, *Science* 356 (2017) 523–527.
- [84] T. Ikuno, J. Zheng, A. Vjunov, M. Sanchez-Sanchez, M.A. Ortuno, D.R. Pahls, J. L. Fulton, D.M. Camaioni, Z.Y. Li, D. Ray, B.L. Mehdi, N.D. Browning, O.K. Farha, J.T. Hupp, C.J. Cramer, L. Gagliardi, J.A. Lercher, Methane oxidation to methanol catalyzed by Cu-Oxo clusters stabilized in NU-1000 metal–organic framework, *J. Am. Chem. Soc.* 139 (2017) 10294–10301.
- [85] Z. Liang, T. Li, M. Kim, A. Asthagiri, J.F. Weaver, Low-temperature activation of methane on the IrO₂(110) surface, *Science* 356 (2017) 299–303.
- [86] L. Yang, J.X. Huang, R. Ma, R. You, H. Zeng, Z.B. Rui, Metal–organic framework-derived IrO₂/CuO catalyst for selective oxidation of methane to methanol, *ACS Energy Lett.* 4 (2019) 2945–2951.
- [87] G.D. Qi, T.E. Davies, A. Nasrallah, M.A. Sainna, A.G.R. Howe, R.J. Lewis, M. Quesne, C.R.A. Catlow, D.J. Willock, Q. He, D. Bethell, M.J. Howard, B. A. Murrer, B. Harrison, C.J. Kiely, X.L. Zhao, F. Deng, J. Xu, G.J. Hutchings, Au-ZSM-5 catalyses the selective oxidation of CH₄ to CH₃OH and CH₃COOH using O₂, *Nat. Catal.* 5 (2022) 45–54.
- [88] P. Kumar, T.A. Al-Attas, J.G. Hu, M.G. Kibria, Single atom catalysts for selective methane oxidation to oxygenates, *ACS Nano* 16 (2022) 8557–8618.
- [89] X. Tang, L. Wang, B. Yang, C. Fei, T.Y. Yao, W. Liu, A. Lou, Q.G. Dai, Y.F. Cai, X. M. Cao, W.C. Zhan, Y.L. Guo, X.Q. Gong, Y. Guo, Direct oxidation of methane to oxygenates on supported single Cu atom catalyst, *Appl. Catal. B: Environ.* 285 (2021) 119827–119835.
- [90] X.J. Cui, H.B. Li, Y. Wang, Y.L. Hu, L. Hua, H.Y. Li, X.W. Han, Q.F. Liu, F. Yang, L. M. He, X.Q. Chen, Q.Y. Li, J.P. Xiao, D.H. Deng, X.H. Bao, Room-temperature methane conversion by graphene-confined single iron, *At. Chem.* 4 (2018) 1–9.
- [91] Y. Kwon, T.Y. Kim, G. Kwon, J. Yi, H. Lee, Selective activation of methane on single-atom catalyst of rhodium dispersed on zirconia for direct conversion, *J. Am. Chem. Soc.* 139 (2017) 17694–17699.
- [92] C. Hammond, M.M. Forde, M.H. Rahim, A.A. Thetford, Q. He, R.L. Jenkins, N. Dimitratos, J.A. Lopez-Sanchez, N.F. Dummer, D.M. Murphy, A.F. Carley, S. H. Taylor, D.J. Willock, E.E. Stangland, J. Kang, H. Hagen, C.J. Kiely, G. J. Hutchings, Direct catalytic conversion of methane to methanol in an aqueous medium by using copper-promoted Fe-ZSM-5, *Angew. Chem. Int. Ed.* 51 (2012) 5129–5133.
- [93] M.H. Rahim, M.M. Forde, R.L. Jenkins, C. Hammond, Q. He, N. Dimitratos, J. A. Lopez-Sanchez, A.F. Carley, S.H. Taylor, D.J. Willock, D.M. Murphy, C.J. Kiely, G. J. Hutchings, Oxidation of methane to methanol with hydrogen peroxide using supported gold-palladium alloy nanoparticles, *Angew. Chem. Int. Ed.* 52 (2013) 1280–1284.
- [94] W.X. Huang, S.R. Zhang, Y. Tang, Y.T. Li, L. Nguyen, Y.Y. Li, J.J. Shan, D. Xiao, R. Gagne, A.I. Frenkel, F. Tao, Low-temperature transformation of methane to methanol on Pd₁O₄ single sites anchored on the internal surface of microporous silicate, *Angew. Chem. Int. Ed.* 55 (2016) 13441–13445.
- [95] K. Harath, X.H. Yu, H. Xiao, J. Li, The key role of support surface hydrogenation in the CH₄ to CH₃OH selective oxidation by a ZrO₂-supported single-atom catalyst, *ACS Catal.* 9 (2019) 8903–8909.
- [96] Y.H. Chin, C. Buda, M. Neurock, E. Iglesia, Reactivity of chemisorbed oxygen atoms and their catalytic consequences during CH₄-O₂ catalysis on supported Pt clusters, *J. Am. Chem. Soc.* 133 (2011) 15958–15978.
- [97] J.H.B. Sattler, I.D. Gonzalez-Jimenez, L. Luo, B.A. Stears, A. Malek, D.G. Barton, B.A. Kilos, M.P. Kaminsky, T.W.G.M. Verhoeven, E.J. Koers, M. Baldus, B. M. Weckhuysen, Platinum-promoted Ga/Al₂O₃ as highly active, selective, and stable catalyst for the dehydrogenation of propane, *Angew. Chem. Int. Ed.* 53 (2014) 9251–9256.
- [98] P. Schwach, X.L. Pan, X.H. Bao, Direct conversion of methane to value-added chemicals over heterogeneous catalysts: challenges and prospects, *Chem. Rev.* 117 (2017) 8497–8520.
- [99] P. Tian, Y.X. Wei, M. Ye, Z.M. Liu, Methanol to olefins (MTO): from fundamentals to commercialization, *ACS Catal.* 5 (2015) 1922–1938.
- [100] U. Olsbye, S. Svelle, M. Bjørge, P. Beato, T.V.W. Janssens, F. Joensen, S. Bordiga, K.P. Lillerud, Conversion of methanol to hydrocarbons: how zeolite cavity and pore size controls product selectivity, *Angew. Chem. Int. Ed.* 51 (2012) 5810–5831.
- [101] P.F. Xie, T.C. Pu, A.M. Nie, S. Hwang, S.C. Purdy, W.J. Yu, D. Su, J. Miller, C. Wang, Nanoceria supported single-atom platinum catalysts for direct methane conversion, *ACS Catal.* 8 (2018) 4044–4048.
- [102] Y.J. Xi, A. Heyden, Direct oxidation of methane to methanol enabled by electronic atomic monolayer-metal support interaction, *ACS Catal.* 9 (2019) 6073–6079.
- [103] H.T. Zhang, C. Liu, P. Liu, Y.H. Hu, Mo₆S₈-based single-metal-atom catalysts for direct methane to methanol conversion, *J. Chem. Phys.* 151 (2019) 024304–024316.

- [104] M.H. Groothaert, P.J. Smeets, B.F. Sels, P.A. Jacobs, R.A. Schoonheydt, Selective oxidation of methane by the bis(μ -oxo)dycopper core stabilized on ZSM-5 and mordenite zeolites, *J. Am. Chem. Soc.* 127 (2005) 1394–1395.
- [105] B.E.R. Snyder, P. Vanelderen, M.L. Bols, S.D. Hallaert, L.H. Böttger, L. Ungur, K. Pierloot, R.A. Schoonheydt, B.F. Sels, E.I. Solomon, The active site of low-temperature methane hydroxylation in iron-containing zeolites, *Nature* 536 (2016) 317–321.
- [106] Z.J. Zuo, P.J. Ramirez, S. Senanayake, P. Liu, J.A. Rodriguez, The low-temperature conversion of methane to methanol on $\text{CeO}_x/\text{Cu}_2\text{O}$ catalysts: water controlled activation of the C-H bond, *J. Am. Chem. Soc.* 138 (2016) 13810–13813.
- [107] Z.Y. Liu, E.W. Huang, I. Orozco, W.J. Liao, R.M. Palomino, N. Rui, T. Duchon, S. Nemsák, D.C. Grinter, M. Mahapatra, P. Liu, J.A. Rodriguez, S.D. Senanayake, Water-promoted interfacial pathways in methane oxidation to methanol on a CeO_2 - Cu_2O catalyst, *Science* 368 (2020) 513–517.
- [108] Q.K. Shen, C.Y. Cao, R.K. Huang, L. Zhu, X. Zhou, Q.H. Zhang, L. Gu, W.G. Song, Single chromium atoms supported on titanium dioxide nanoparticles for synergistic catalytic methane conversion under mild conditions, *Angew. Chem.* 132 (2020) 1232–1235.
- [109] S.X. Bai, F.F. Liu, B.L. Huang, F. Li, H.P. Lin, T. Wu, M.Z. Sun, J.B. Wu, Q. Shao, Y. Xu, X.Q. Huang, High-efficiency direct methane conversion to oxygenates on a cerium dioxide nanowires supported rhodium single-atom catalyst, *Nat. Commun.* 11 (2020) 954–962.
- [110] F.B. Gu, X.T. Qin, M.W. Li, Y. Xu, S. Hong, M.Y. Ouyang, G. Giannakakis, S.F. Cao, M. Peng, J.L. Xie, M. Wang, D.M. Han, D.Q. Xiao, X.Y. Wang, Z.H. Wang, D. Ma, Selective catalytic oxidation of methane to methanol in aqueous medium over copper cations promoted by atomically dispersed rhodium on TiO_2 , *Angew. Chem.* 134 (2022), e202201540.
- [111] M.S.A.S. Shah, C. Oh, H. Park, Y.J. Hwang, M. Ma, J.H. Park, Catalytic oxidation of methane to oxygenated products: recent advancements and prospects for electrocatalytic and photocatalytic conversion at low temperatures, *Adv. Sci.* 7 (2020) 2001946–2200169.
- [112] X.X. Chen, Y.P. Li, X.Y. Pan, D. Cortie, X.T. Huang, Z.G. Yi, Photocatalytic oxidation of methane over silver decorated zinc oxide nanocatalysts, *Nat. Commun.* 7 (2016) 12273–12280.
- [113] Y.Y. Fan, W.C. Zhou, X.Y. Qiu, H.D. Li, Y.B. Jiang, Z.H. Sun, D.X. Han, L. Niu, Z. Y. Tang, Selective photocatalytic oxidation of methane by quantum-sized bismuth vanadate, *Nat. Sustain.* 4 (2021) 509–515.
- [114] Y. Zeng, Z.Y. Tang, X.Y. Wu, A.H. Huang, X. Luo, G.Q. Xu, Y.F. Zhu, S.L. Wang, Photocatalytic oxidation of methane to methanol by tungsten trioxide-supported atomic gold at room temperature, *Appl. Catal. B: Environ.* 306 (2022) 120919–120926.
- [115] X. Tang, L. Wang, B. Yang, C. Fei, T.Y. Yao, W. Liu, Y. Lou, Q.G. Dai, Y.F. Cai, X. M. Cao, W.C. Zhan, Y.L. Guo, X.Q. Gong, Y. Guo, Direct oxidation of methane to oxygenates on supported single Cu atom catalyst, *Appl. Catal. B: Environ.* 285 (2021) 119827–119835.
- [116] M. Huang, S.Y. Zhang, B. Wu, Y. Wei, X. Yu, Y.P. Gan, T.J. Lin, F. Yu, F.F. Sun, Z. Jiang, L.S. Zhong, Selective photocatalytic oxidation of methane to oxygenates over $\text{Cu}-\text{W}-\text{TiO}_2$ with significant carrier traps, *ACS Catal.* 12 (2022) 9515–9525.
- [117] A. Abad, P. Concepcion, A. Corma, H. Garcia, A collaborative effect between gold and support induces the selective oxidation of alcohols, *Angew. Chem. Int. Ed.* 44 (2005) 4066–4069.
- [118] C.P. Vinod, K. Wilson, A.F. Lee, Recent advances in the heterogeneously catalysed aerobic selective oxidation of alcohols, *J. Chem. Technol. Biotechnol.* 86 (2011) 161–171.
- [119] Q.H. Zhang, W.P. Deng, Y. Wang, Effect of size of catalytically active phases in the dehydrogenation of alcohols and the challenging selective oxidation of hydrocarbons, *Chem. Commun.* 47 (2011) 9275–9292.
- [120] T. Mallat, A. Baiker, Oxidation of alcohols with molecular oxygen on solid catalysts, *Chem. Rev.* 104 (2004) 3037–3058.
- [121] C.Y. Ma, W.J. Xue, J.J. Li, W. Xing, Z.P. Hao, Mesoporous carbon-confined Au catalysts with superior activity for selective oxidation of glucose to gluconic acid, *Green Chem.* 15 (2013) 1035–1041.
- [122] J. Chen, Q.H. Zhang, Y. Wang, Wan, L. H, Size-dependent catalytic activity of supported palladium nanoparticles for aerobic oxidation of alcohols, *Adv. Synth. Catal.* 350 (2008) 453–464.
- [123] B.R. Cuenya, Metal nanoparticle catalysts beginning to shape-up, *Acc. Chem. Res.* 46 (2013) 1682–1691.
- [124] S.W. Cao, F. Tao, Y. Tang, Y.T. Li, J.G. Yu, Size- and shape-dependent catalytic performances of oxidation and reduction reactions on nanocatalysts, *Chem. Soc. Rev.* 45 (2016) 4747–4765.
- [125] C.M. Zhou, Y.T. Chen, Z. Guo, X. Wang, Y.H. Yang, Promoted aerobic oxidation of benzyl alcohol on CNT supported platinum by iron oxide, *Chem. Commun.* 47 (2011) 7473–7475.
- [126] S. Mostafa, F. Behafarid, J.R. Croy, L.K. Ono, L. Li, J.C. Yang, A.I. Frenkel, B. R. Cuenya, Shape-dependent catalytic properties of Pt nanoparticles, *J. Am. Chem. Soc.* 132 (2010) 15714–15719.
- [127] H. Mistry, F. Behafarid, E. Zhou, L.K. Ono, L. Zhang, B.R. Cuenya, Shape-dependent catalytic oxidation of 2-butanol over Pt nanoparticles supported on γ - Al_2O_3 , *ACS Catal.* 4 (2014) 109–115.
- [128] W.X. Sun, S.P. Wu, Y.W. Lu, Y.X. Wang, Q.E. Cao, W.H. Fang, Effective control of particle size and electron density of Pd/C and SnPd/C nanocatalysts for vanillin production via base-free oxidation, *ACS Catal.* 10 (2020) 7699–7709.
- [129] Q.H. Tang, X.N. Huang, C.M. Wu, P.Z. Zhao, Y.T. Chen, Y.H. Yang, Structure and catalytic properties of K-doped manganese oxide supported on alumina, *J. Mol. Catal. A: Chem.* 306 (2009) 48–53.
- [130] G.F. Zhao, F. Yang, Z.J. Chen, Q.F. Liu, Y.J. Ji, Y. Zhang, Z.Q. Niu, J.J. Mao, X. H. Bao, P.J. Hu, Y.D. Li, Metal/oxide interfacial effects on the selective oxidation of primary alcohols, *Nat. Commun.* 8 (2017) 14039–14046.
- [131] F. Polo-Garzon, T.F. Blum, Z.H. Bao, K. Wang, V. Fung, Z.N. Huang, E.E. Bickel, D. Jiang, M.F. Chi, Z.L. Wu, In situ strong metal–support interaction (SMSI) affects catalytic alcohol conversion, *ACS Catal.* 11 (2021) 1938–1945.
- [132] H.L. Liu, Y.L. Liu, Y.W. Li, Z.Y. Tang, H.F. Jiang, Metal-organic framework supported gold nanoparticles as a highly active heterogeneous catalyst for aerobic oxidation of alcohols, *J. Phys. Chem. C* 114 (2010) 13362–13369.
- [133] H.L. Liu, L.N. Chang, C.H. Bai, L.Y. Chen, R. Luque, Y.W. Li, Controllable encapsulation of “clean” metal clusters within MOFs through kinetic modulation: towards advanced heterogeneous nanocatalysts, *Angew. Chem. Int. Ed.* 55 (2016) 5019–5023.
- [134] S.F.J. Hackett, R.M. Brydson, M.H. Gass, I. Harvey, A.D. Newman, K. Wilson, A. F. Lee, High-activity, single-site mesoporous Pd/ Al_2O_3 catalysts for selective aerobic oxidation of allylic alcohols, *Angew. Chem. Int. Ed.* 46 (2007) 8593–8596.
- [135] T.B. Li, F. Liu, Y. Tang, L. Li, S. Miao, Y. Su, J.Y. Zhang, J.H. Huang, H. Sun, M. Haruta, A.Q. Wang, B.T. Qiao, J. Li, T. Zhang, Maximizing interfacial sites by single-atom catalyst for solvent-free selective oxidation of primary alcohol, *Angew. Chem. Int. Ed.* 57 (2018) 7795–7800.
- [136] J.Q. Li, S.Y. Zhao, L.J. Zhang, S.P. Jiang, S.Z. Yang, S.B. Wang, H.Q. Sun, B. Johannessen, S.M. Liu, Cobalt single atoms embedded in nitrogen-doped graphene for selective oxidation of benzyl alcohol by activated peroxymonosulfate, *Small* 17 (2021) 2004579–2004586.
- [137] Z.J. Li, H.H. Li, Z.N. Yang, X.W. Lu, S.Q. Ji, M.Y. Zhang, J.H. Horton, H.H. Ding, Q. Xu, J.F. Zhu, J. Yu, Facile synthesis of single iron atoms over MoS_2 nanosheets via spontaneous reduction for highly efficient selective oxidation of alcohols, *Small* 18 (2022) 2201–2210.
- [138] Z.J. Li, T.T. Fan, H.H. Li, X.W. Lu, S.Q. Ji, J.W. Zhang, J.H. Horton, Q. Xu, J. F. Zhu, Atomically defined undercoordinated copper active sites over nitrogen-doped carbon for aerobic oxidation of alcohols, *Small* 18 (2022) 2106614–2106622.
- [139] P.Y. Xin, J. Li, Y. Xiong, X. Wu, J.C. Dong, W.X. Chen, Y. Wang, L. Gu, J. Luo, Rong, P. H. C. Chen, Q. Peng, D.S. Wang, Y.D. Li, Revealing the active species for aerobic alcohol oxidation by using uniform supported palladium catalysts, *Angew. Chem.* 130 (2018) 4732–4736.
- [140] Y.H. Fu, L. Sun, H. Yang, L. Xu, F.M. Zhang, W.D. Zhu, Visible-light-induced aerobic photocatalytic oxidation of aromatic alcohols to aldehydes over Ni-doped NH_2 -MIL-125(Ti), *Appl. Catal. B: Environ.* 187 (2016) 212–217.
- [141] M. Bellardita, E.I. García-López, G. Marci, I. Krivtsov, J.R. García, L. Palmisano, Selective photocatalytic oxidation of aromatic alcohols in water by using P doped C_3N_4 , *Appl. Catal. B: Environ.* 220 (2018) 222–233.
- [142] F. Zhang, J. Ma, Y. Tan, G. Yu, H.X. Qin, L.R. Zheng, H.B. Liu, R. Li, Construction of porphyrin porous organic cage as a support for single cobalt atoms for photocatalytic oxidation in visible light, *ACS Catal.* 12 (2022) 5827–5833.
- [143] J.Q. Li, S.Y. Zhao, L.J. Zhang, S.P. Jiang, S.Z. Yang, S.B. Wang, H.Q. Sun, B. Johannessen, S.M. Liu, Cobalt single atoms embedded in nitrogen-doped graphene for selective oxidation of benzyl alcohol by activated peroxymonosulfate, *Small* 17 (2021) 2004579–2004586.
- [144] S.B. Tian, Q. Fu, W.X. Chen, Q.C. Feng, Z. Chen, J. Zhang, W.C. Cheong, R. Yu, L. Gu, J.C. Dong, J. Luo, C. Chen, Q. Peng, C. Drax, D.S. Wang, Y.D. Li, Carbon nitride supported Fe_2 cluster catalysts with superior performance for alkene epoxidation, *Nat. Commun.* 9 (2018) 2353–2359.
- [145] C. Weerakkody, S. Biswas, W.Q. Song, J.K. He, N. Wasalathanthri, S. Dissanayake, D.A. Kriz, B. Dutta, S.L. Suib, Controllable synthesis of mesoporous cobalt oxide for peroxide free catalytic epoxidation of alkenes under aerobic conditions, *Appl. Catal. B: Environ.* 221 (2018) 681–690.
- [146] A.J.F. Hoof, I.A.W. Pilot, H. Friedrich, E.J.M. Hensen, Reversible restructuring of silver particles during ethylene epoxidation, *ACS Catal.* 8 (2018) 11794–11800.
- [147] M. Huš, A. Hellman, Ethylene epoxidation on Ag(100), Ag(110), Ag(111): a joint Ab initio and kinetic Monte Carlo study and comparison with experiments, *ACS Catal.* 9 (2019) 1183–1196.
- [148] Y. Lei, F. Mehmood, S. Lee, J. Greeley, B. Lee, S. Seifert, R.E. Winans, W. Elam, R. J. Meyer, P.C. Redfern, D. Teschner, R. Schlog, M.J. Pellin, L.A. Curtiss, S. Vajda, Increased silver activity for direct propylene epoxidation via subnanometer size effects, *Science* 328 (2010) 224–228.
- [149] S. Bawaked, N.F. Dummer, N. Dimitratos, D. Bethell, Q. He, C.J. Kiely, G. J. Hutchings, Solvent-free selective epoxidation of cyclooctene using supported gold catalysts, *Green Chem.* 11 (2009) 1037–1044.
- [150] R.L. Cropley, F.J. Williams, O.P.H. Vaughan, A.J. Urquhart, M.S. Tikhov, R. M. Lambert, Copper is highly effective for the epoxidation of a “difficult” alkene, whereas silver is not, *Surf. Sci.* 578 (2005) 85–88.
- [151] A. Bhaumik, T. Tatsumi, Organically modified titanium-rich Ti-MCM-41, efficient catalysts for epoxidation reactions, *J. Catal.* 189 (2000) 31–39.
- [152] K. Kamata, K. Yonehara, Y. Sumida, K. Hirata, S. Nojima, N. Mizuno, Efficient heterogeneous epoxidation of alkenes by a supported tungsten oxide catalyst, *Angew. Chem. Int. Ed.* 50 (2011) 12062–12066.
- [153] Y.R. Shen, P.P. Jiang, P.T. Wai, Q. Gu, W.J. Zhang, Recent progress in application of molybdenum-based catalysts for epoxidation of alkenes, *Catal* 9 (2019) 31–57.
- [154] Global and China Ethylene Oxide (EO) Industry Report, 2017–2021. *Res. China* 2017, 137.
- [155] H.L. Yang, C.Y. Ma, X. Zhang, Y. Li, J. Cheng, Z.P. Hao, Understanding the active sites of Ag/zeolites and deactivation mechanism of ethylene catalytic oxidation at room temperature, *ACS Catal.* 8 (2018) 1248–1258.

- [156] T.C. Pu, H.J. Tian, M.E. Ford, S. Rangarajan, I.E. Wachs, Overview of selective oxidation of ethylene to ethylene oxide by Ag catalysts, *ACS Catal.* 9 (2019) 10727–10750.
- [157] H.L. Yang, C.Y. Ma, Z.S. Zhang, Z.P. Hao, Fluorine-enhanced Pt/ZSM-5 catalysts for low temperature oxidation of ethylene, *Catal. Sci. Technol.* 8 (2018) 1988–1996.
- [158] H.L. Yang, C.Y. Ma, Y. Li, J.H. Wang, X. Zhang, G. Wang, N.L. Qiao, Y.G. Sun, J. Cheng, Z.P. Hao, Synthesis, characterization and evaluations of the Ag/ZSM-5 for ethylene oxidation at room temperature: investigating the effect of water and deactivation, *Chem. Eng. J.* 347 (2018) 808–818.
- [159] P. Christopher, S. Linic, Engineering selectivity in heterogeneous catalysis: Ag nanowires as selective ethylene epoxidation catalysts, *J. Am. Chem. Soc.* 130 (2008) 11264–11265.
- [160] A. Ramirez, J.L. Hueso, H. Suarez, R. Mallada, A. Ibarra, S. Irusta, J. Santamaria, A nanoarchitecture based on silver and copper oxide with an exceptional response in the chlorine-promoted epoxidation of ethylene, *Angew. Chem. Int. Ed.* 55 (2016) 11158–11161.
- [161] P. Christopher, S. Linic, Shape- and size-specific chemistry of Ag nanostructures in catalytic ethylene epoxidation, *ChemCatChem* 2 (2010) 78–83.
- [162] E.A. Carbonio, T.C.R. Rocha, A.Y. Klyushin, I. Pis, E. Magnano, S. Nappini, S. Piccinin, A.K. Gericke, R. Schlögl, T.E. Jones, Are multiple oxygen species selective in ethylene epoxidation on silver? *Chem. Sci.* 9 (2018) 990–998.
- [163] T.E. Jones, R. Wyrwich, S. Böcklein, E.A. Carbonio, M. Greiner, Y.A. Klyushin, W. Moritz, A. Locatelli, T.O. Mente, M.A. Niño, A. Knop-Gericke, R. Schlögl, S. Günther, J. Wintterlin, S. Piccinin, The selective species in ethylene epoxidation on silver, *ACS Catal.* 8 (2018) 3844–3852.
- [164] Y. Xu, J. Greeley, M. Mavrikakis, Effect of subsurface oxygen on the reactivity of the Ag(111) surface, *J. Am. Chem. Soc.* 127 (2005) 12823–12827.
- [165] A.K. Sinha, S. Seelan, S. Tsubota, M. Haruta, Catalysis by gold nanoparticles: epoxidation of propene, *Top. Catal.* 29 (2004) 95–102.
- [166] Taramasso, M.; Perego, G.; Notari, B. Preparation of porous crystalline synthetic materials comprised of silicon and titanium oxides. US Pat. 1983. 4410501.
- [167] M.G. Clerici, G. Bellussi, U. Romano, *J. Catal.* 129 (1991) 159–167.
- [168] T. Hayashi, K. Tanaka, M. Haruta, Selective vapor-phase epoxidation of propylene over Au/TiO₂ catalysts in the presence of oxygen and hydrogen, *J. Catal.* 178 (1998) 566–575.
- [169] M. Haruta, B.S. Uphade, S. Tsubota, A. Miyamoto, Selective oxidation of propylene over gold deposited on titanium-based oxides, *Res. Chem. Intermed.* 24 (1998) 329–336.
- [170] B.S. Uphade, T. Akita, T. Nakamura, M. Haruta, Vapor-phase epoxidation of propene using H₂ and O₂ over Au/Ti-MCM-48, *J. Catal.* 209 (2002) 331–340.
- [171] M.P. Kapoor, A.K. Sinha, S. Seelan, S. Inagaki, S. Tsubota, H. Yoshida, M. Haruta, Hydrophobicity induced vapor-phase oxidation of propene over gold supported on titanium incorporated hybrid mesoporous silsesquioxane, *Chem. Commun.* (2002) 2902–2903.
- [172] S.L. Chen, D. Li, T. Cao, W.X. Huang, Size-dependent structures and catalytic performances of Au/TiO₂-(001) catalysts for propene epoxidation, *J. Phys. Chem. C* 124 (28) (2020) 15264–15274.
- [173] B.S. Uphade, M. Okumura, S. Tsubota, M. Haruta, Effect of physical mixing of CsCl with Au/Ti-MCM-41 on the gas-phase epoxidation of propene using H₂ and O₂: drastic depression of H₂ consumption, *Appl. Catal. A: Gen.* 190 (2000) 43–50.
- [174] Q.Q. Zhang, X. Zhao, J. Yang, M.Y. Zheng, W.L. Fan, Theoretical insights into propene epoxidation on Au₇/anatase TiO₂-(001) catalysts: effect of the interface and reaction atmosphere, *J. Phys. Chem. C* 123 (2019) 3568–3578.
- [175] B. Liu, P. Wang, A. Lopes, L. Jin, W. Zhong, Y. Pei, S.L. Suib, J. He, Au–carbon electronic interaction mediated selective oxidation of styrene, *ACS Catal.* 7 (2017) 3483–3488.
- [176] J.Y. Liu, X.Y. Ji, J. Shi, L.X. Wang, P.M. Jian, X.D. Yan, D. Wang, Experimental and theoretical investigation of the tuning of electronic structure in SnO₂ via Co doping for enhanced styrene epoxidation catalysis, *Catal. Sci. Technol.* 12 (2022) 1499–1511.
- [177] M. Hosseini-Sarvari, Z. Bazayr, Selective visible-light photocatalytic aerobic oxidation of alkenes to epoxides with Pd/ZnO Nanoparticles, *ChemistrySelect* 5 (2020) 8853–8857.
- [178] H.L. Yang, X. Zhang, Y. Yu, X. Chen, C. Chen, Y.D. Li, Manganese vacancy-confined single-atom Ag in cryptomelane nanorods for efficient wacker oxidation of styrene derivatives, *Chem. Sci.* 12 (2021) 6099–6106.
- [179] X. Liu, Y. Yang, M.M. Chu, T. Duan, C.G. Meng, Y. Han, Defect stabilized gold atoms on graphene as potential catalysts for ethylene epoxidation: a first-principles investigation, *Catal. Sci. Technol.* 6 (2016) 1632–1641.
- [180] C.G. Liu, M.X. Jiang, Z.M. Su, Computational study on M₁/POM single-atom catalysts (M = Cu, Zn, Ag, and Au; POM = [PW₁₂O₄₀]³⁻): metal–support interactions and catalytic cycle for alkene epoxidation, *Inorg. Chem.* 56 (2017) 10496–10504.
- [181] Z. Lu, X.Y. Liu, B. Zhang, Z.R. Gan, S.W. Tang, L. Ma, T.P. Wu, G.J. Nelson, Y. Qin, C.H. Turner, Y. Lei, Structure and reactivity of single site Ti catalysts for propylene epoxidation, *J. Catal.* 377 (2019) 419–428.
- [182] W.S. Lee, M.C. Akatay, E.A. Stach, F.H. Ribeiro, W.N. Delgass, Reproducible preparation of Au/TS-1 with high reaction rate for gas phase epoxidation of propylene, *J. Catal.* 287 (2012) 178–189.
- [183] X.Y. Chen, S.L. Chen, A.P. Jia, J.Q. Lu, W.X. Huang, Gas phase propylene epoxidation over Au supported on titanosilicates with different Ti chemical environments, *Appl. Surf. Sci.* 393 (2017) 11–22.
- [184] G. Mul, A. Zwijnenburg, B.V.D. Linden, M. Makkee, J.A. Moulijn, Stability and selectivity of Au/TiO₂ and Au/TiO₂/SiO₂ catalysts in propene epoxidation: an in situ FT-IR study, *J. Catal.* 201 (2001) 128–137.
- [185] H.L. Yang, Q.G. Liu, C. Chen, Isolated single-atom ruthenium anchored on beta zeolite as an efficient heterogeneous catalyst for styrene epoxidation, *ChemNanoMat* 6 (2020) 1647–1651.
- [186] S.B. Tian, C. Peng, J.C. Dong, Q. Xu, Z. Chen, D. Zhai, Y. Wang, L. Gu, P. Hu, H. H. Duan, D.S. Wang, Y.D. Li, High-loading single-atomic-site silver catalysts with an Ag₁–C₂N₂ structure showing superior performance for epoxidation of styrene, *ACS Catal.* 11 (2021) 4946–4954.
- [187] Y. Xiong, W.M. Sun, P.Y. Xin, W.X. Chen, X.S. Zheng, W.S. Yan, L.R. Zheng, J. C. Dong, J. Zhang, D.S. Wang, Y.D. Li, Gram-scale synthesis of high-loading single-atomic-site Fe catalysts for effective epoxidation of styrene, *Adv. Mater.* 32 (2020) 2000896–2000903.
- [188] W.J. Li, G.J. Wu, W.D. Hu, J. Dang, C.M. Wang, X.F. Weng, I.D. Silva, P. Manuel, S.H. Yang, N.J. Guan, L.D. Li, Direct propylene epoxidation with molecular oxygen over cobalt containing zeolites, *J. Am. Chem. Soc.* 144 (2022) 4260–4268.
- [189] H.J. Freund, G. Meijer, M. Scheffler, R. Schlögl, M. Wolf, CO oxidation as a prototypical reaction for heterogeneous processes, *Angew. Chem. Int. Ed.* 50 (2011) 10064–10094.
- [190] P. Gawade, B. Bayram, A.M.C. Alexander, U.S. Ozkan, Preferential oxidation of CO (PROX) over CO_x/CeO₂ in hydrogen-rich streams: effect of cobalt loading, *Appl. Catal. B: Environ.* 128 (2012) 21–30.
- [191] S.B. Royer, D. Duprez, Catalytic oxidation of carbon monoxide over transition metal oxides, *ChemCatChem* 3 (2011) 24–65.
- [192] S.Y. Yamamoto, C.M. Surko, M.B. Maple, R.K. Pina, Spatiotemporal dynamics of oscillatory heterogeneous catalysis: CO oxidation on platinum, *J. Chem. Phys.* 102 (1995) 8614–8625.
- [193] H. Over, M. Muhler, Catalytic CO oxidation over Ruthenium-Bridging the Pressure Gap, *Prog. Surf. Sci.* 72 (2003) 3–17.
- [194] H.J. Freund, G. Meijer, M. Scheffler, R. Schlögl, M. Wolf, CO oxidation as a prototypical reaction for heterogeneous processes, *Angew. Chem. Int. Ed.* 50 (2011) 10064–10094.
- [195] M.J. Haruta, N. Yamada, T. Kobayashi, Gold catalysts prepared by coprecipitation for low-temperature oxidation of hydrogen and of carbon monoxide, *J. Catal.* 115 (1989) 301–309.
- [196] M.J. Haruta, N. Yamada, T. Kobayashi, Low-temperature oxidation of CO over gold support on TiO₂, α-Fe₂O₃, and Co₃O₄, *J. Catal.* 144 (1993) 175–192.
- [197] T. Ishida, T. Murayama, A. Taketoshi, M. Haruta, Importance of size and contact structure of gold nanoparticles for the genesis of unique catalytic processes, *Chem. Rev.* 120 (2020) 464–525.
- [198] Z.P. Hao, L.D. An, H.L. Wang, Mechanism of gold activation in ferric oxide and its compost oxides supported gold catalysts for low-temperature CO oxidation, *Chin. Sci. B* 44 (2001) 596–605.
- [199] Z.P. Hao, S.C. Zhang, Z.M. Liu, H.P. Zhang, In situ IR pulse reaction and TPD-ITD study of catalytic performance of room-temperature carbon monoxide oxidation on supported gold catalysts, *J. Environ. Sci.* 14 (2002) 489–494.
- [200] A.A. Herzog, C.J. Kiely, A.F. Carley, P. Landon, G.J. Hutchings, Identification of active gold nanoclusters on iron oxide supports for CO oxidation, *Science* 321 (2008) 1331–1335.
- [201] Q. He, S.J. Freakeley, J.K. Edwards, A.F. Carley, A.Y. Borisevich, Y. Mineo, M. Haruta, G.J. Hutchings, C.J. Kiely, Population and hierarchy of active species in gold iron oxide catalysts for carbon monoxide oxidation, *Nat. Commun.* 7 (2016) 12905–12912.
- [202] B. Yoon, H. Hakkinen, U. Landman, A.S. Worz, J.M. Antonietti, S. Abbet, K. Judai, U. Heiz, Charging effects on bonding and catalyzed oxidation of CO on Au₈ clusters on MgO, *Science* 307 (2005) 403–407.
- [203] C. Harding, V. Habibpour, S. Kunz, A.N.S. Farnbacher, U. Heiz, B. Yoon, U. Landman, Control and manipulation of gold nanocatalysis: effects of metal oxide support thickness and composition, *J. Am. Chem. Soc.* 131 (2009) 538–548.
- [204] W.E. Kaden, T. Wu, W.A. Kunkel, S.L. Anderson, Electronic structure controls reactivity of size-selected Pd clusters adsorbed on TiO₂ surfaces, *Science* 326 (2006) 826–829.
- [205] U. Heiz, A. Sanchez, S. Abbet, W.D. Schneider, Catalytic oxidation of carbon monoxide on monodispersed platinum clusters: each atom counts, *J. Am. Chem. Soc.* 121 (1999) 3214–3217.
- [206] A.M. Pennington, C.L. Pitman, P.A. DeSario, T.H. Brintlinger, S. Jeon, R.B. Balow, J.J. Pietron, R.M. Stroud, D.R. Rolison, Photocatalytic CO oxidation over nanoparticulate Au-modified TiO₂ aerogels: the importance of size and intimacy, *ACS Catal.* 10 (2020) 14834–14846.
- [207] W. Li, L.Y. Du, C.J. Jia, R. Si, Support effect of zinc tin oxide on gold catalyst for CO oxidation reaction, *Chin. J. Catal.* 37 (2016) 1702–1711.
- [208] Z.R. Mansley, R.J. Paull, L. Savereide, S. Tatro, E.P. Greenstein, A. Gosavi, E. Cheng, J.G. Wen, K.R. Poeppelmeier, J.M. Notestein, L.D. Marks, Identifying support effects in Au-catalyzed CO oxidation, *ACS Catal.* 11 (2021) 11921–11928.
- [209] H. Ha, H. An, M. Yoo, J. Lee, H.Y. Kim, Catalytic CO oxidation by CO-saturated Au nanoparticles supported on CeO₂: effect of CO coverage, *J. Phys. Chem. C* 121 (2017) 26895–26902.
- [210] M. Dat, M. Okumura, S. Tsubota, M. Haruta, Vital role of moisture in the catalytic activity of supported gold nanoparticles, *Angew. Chem.* 116 (2004) 2181–2184.
- [211] C.L. Wang, X.K. Gu, H. Yan, Y. Lin, J.J. Li, D.D. Liu, W.X. Li, J.L. Lu, Water-mediated Mars-Van Krevelen mechanism for CO oxidation on ceria supported single-atom Pt₁ catalyst, *ACS Catal.* 7 (2017) 887–891.
- [212] O. Pozdnyakova, D. Teschner, J. Kröhnert, B. Steinhauer, H. Sauer, L. Toth, F.C. Jentoft, A. Knop-Gericke, Z. Paál, R. Schlögl, Preferential CO oxidation in hydrogen (PROX) on ceria-supported catalysts, Part I: oxidation state and surface species on Pt/CeO₂ under reaction conditions, *J. Catal.* 237 (2006) 1–16.

- [213] S. Kunz, F.F. Schweinberger, V. Habibpour, M. Rottgen, C. Harding, M. Arenz, U. Heiz, Temperature dependent CO oxidation mechanisms on size-selected clusters, *J. Phys. Chem. C* 114 (2010) 1651–1654.
- [214] M.J. Kahlich, H.A. Gasteiger, R.J. Behm, Kinetics of the selective CO oxidation in H₂-rich gas on Pt/Al₂O₃, *J. Catal.* 171 (1997) 93–105.
- [215] A. Martínez-Arias, D. Gamarra, M. Fernández-García, A. Hornés, C. Belver, Spectroscopic study on the nature of active entities in copper–ceria CO-PROX catalysts, *Top. Catal.* 52 (2009) 1425–1432.
- [216] B.T. Qiao, J.X. Liang, A.Q. Wang, J.Y. Liu, T. Zhang, Single atom gold catalysts for low-temperature CO oxidation, *Chin. J. Catal.* 37 (2016) 1580–1586.
- [217] B.T. Qiao, J.X. Liang, A.Q. Wang, C.Q. Xu, J. Li, T. Zhang, J.Y. Liu, Ultrastable single-atom gold catalysts with strong covalent metal-support interaction (CMSI), *Nano Res.* 8 (2015) 2913–2924.
- [218] B.T. Qiao, J.X. Liu, Y.G. Wang, Q.Q. Lin, X.Y. Liu, A.Q. Wang, J. Li, T. Zhang, J. Y. Liu, Highly efficient catalysis of preferential oxidation of CO in H₂-rich stream by gold single-atom catalysts, *ACS Catal.* 5 (2015) 6249–6254.
- [219] A.J. Therrien, A.J.R. Hensley, M.D. Marcinkowski, R.Q. Zhang, F.R. Lucci, B. Coughlin, A.C. Schilling, J.S. McEwen, E.C.H. Sykes, An atomic-scale view of single-site Pt catalysis for low-temperature CO oxidation, *Nat. Catal.* 1 (2018) 192–198.
- [220] B.T. Qiao, A.Q. Wang, X.F. Yang, L.F. Allard, Z. Jiang, Y.T. Cui, J.Y. Liu, J. Li, T. Zhang, Single-atom catalysis of CO oxidation using Pt₁/FeO_x, *Nat. Chem.* 3 (2011) 634–641.
- [221] M. Moses-DeBusk, M. Yoon, L.F. Allard, D.R. Mullins, Z.L. Wu, X.F. Yang, G. Veith, G.M. Stocks, C.K. Narula, CO oxidation on supported single Pt atoms: experimental and ab initio density functional studies of CO interaction with Pt atom on θ -Al₂O₃(010) surface, *J. Am. Chem. Soc.* 135 (2013) 12634–12645.
- [222] H.L. Yang, Y. Wu, Z.W. Zhuang, Y. Li, C. Chen, Factors affecting the catalytic performance of nano-catalysts, *Chin. J. Chem.* 40 (2022) 515–523.
- [223] W.M. Wan, J.L. Geiger, N. Berdunov, M.L. Luna, S.W. Chee, N. Daelman, N. López, S. Shaikhutdinov, B.R. Cuenya, Highly stable and reactive platinum single atoms on oxygen plasma-functionalized CeO₂ surfaces: nanostructuring and peroxo effects, *Angew. Chem.* 134 (2022), e202112640.
- [224] C. Mochizuki, Y. Inomata, S. Yasumura, M.Y. Lin, A. Taketoshi, T. Honma, N. Sakaguchi, M. Haruta, K. Shimizu, T. Ishida, T. Murayam, Defective NiO as a stabilizer for Au single-atom catalysts, *ACS Catal.* 12 (2022) 6149–6158.
- [225] J. Mosrati, A.M. Abdel-Mageed, T.H.Y. Vuong, R. Grauke, S. Bartling, N. Rockstroh, H. Atia, U. Armbruster, S. Wohlrab, J. Rabeah, A. Brückner, Tiny species with big impact: high activity of Cu single atoms on CeO₂-TiO₂ deciphered by *Operando* spectroscopy, *ACS Catal.* 11 (2021) 10933–10949.
- [226] D. Jiang, G. Wan, C.E. García-Vargas, L.Z. Li, X.I. Pereira-Hernandez, C. Wang, Y. Wang, Elucidation of the active sites in single-atom Pd₁/CeO₂ catalysts for low-temperature CO oxidation, *ACS Catal.* 10 (2020) 11356–11364.
- [227] Y.W. Li, Y.X. Chen, S.D. House, S. Zhao, Z. Wahab, J.C. Yang, R.C. Jin, Interface engineering of gold nanoclusters for CO oxidation catalysis, *ACS Appl. Mater. Interfaces* 10 (2018) 29425–29434.
- [228] B.N. Zope, D.D. Hibbitts, M. Neurock, R.J. Davis, Reactivity of the gold/water interface during selective oxidation catalysis, *Science* 330 (2010) 74–78.
- [229] C.J. Wrasman, A.R. Riscoe, H. Lee, M. Cargnello, Dilute Pd/Au alloys replace Au/TiO₂ interface for selective oxidation reactions, *ACS Catal.* 10 (2020) 1716–1720.
- [230] Y.L. Zhang, J.Y. Zhang, B.S. Zhang, R. Si, B. Han, F. Hong, Y.M. Niu, L. Sun, L. Li, B.T. Qiao, K.J. Sun, J.H. Huang, M. Haruta, Boosting the catalysis of gold by O₂ activation at Au-SiO₂ interface, *Nat. Commun.* 11 (2020) 558–567.
- [231] J.S. Woertink, P.J. Smeets, M.H. Groothaert, M.A. Vance, B.F. Sels, R. A. Schoonheydt, E.I. Solomon, A [Cu₂O]²⁺ Core in Cu-ZSM-5, the Active Site in the Oxidation of Methane to Methanol, *Proc. Natl. Acad. Sci. USA* 106 (2009) 18908–18913.
- [232] D. Palagin, A. Knorpp, A.B. Pinar, M. Ranocchiari, J.A.V. Bokhoven, Assessing relative stability of copper oxide clusters as active sites of CuMOR zeolite for methane to methanol conversion: size matters? *Nanoscale* 9 (2017) 1144–1153.